University of South Bohemia in České Budějovice

Faculty of Science

Molecular, biochemical, and structural characterization of secreted ferritin II from *Ixodes ricinus*

Master thesis

Bc. Anna Koutská

Supervisor: prof. Mgr. Ivana Kutá Smatanová, Ph.D.

Supervisor-specialists: RNDr. Petr Kopáček, CSc., Mgr. Petra Havlíčková

České Budějovice 2023

Koutská, A., 2023: Molecular, biochemical, and structural characterization of secreted ferritin II from *Ixodes ricinus*. Mgr. Thesis, in English. – 63 p., Faculty of Science, University of South Bohemia, České Budějovice, Czech Republic.

Annotation

The aim of this master thesis is to design and produce correctly folded recombinant ferritin II from *Ixodes ricinus*. Ferritin II is considered to be a promising candidate for developing an anti-tick vaccine. Ferritin II was cloned into several vectors and *E. coli* competent cells were used for production of insoluble ferritin II, which was then isolated from inclusion bodies for following structural studies and determination of ferritin II role in ticks´ metabolism of iron.

Prohlašuji, že jsem autorem této kvalifikační práce a že jsem ji vypracoval(a) pouze s použitím pramenů a literatury uvedených v seznamu použitých zdrojů.

České Budějovice, 13.4. 2023

…….

Bc. Anna Koutská

Acknowledgements:

First, I would like to thank my supervisor prof. Mgr. Ivana Kutá Smatanová, Ph.D. for the pleasant atmosphere in the lab, as well as for her valuable advice and unwavering support. I would also like to express my gratitude to my supervisor-specialist Mgr. Petra Havlíčková for her willingness, supervision, guidance, and support during the lab work. Furthermore, I would like to thank RNDr. Petr Kopáček, CSc. and RNDr. Zdeněk Franta, Ph.D. for teaching me new techniques and their valuable advice that helped me to advance the task.

This work could not be possible without the construct provided by RNDr. Petr Kopáček, CSc. and his colleagues and final protein measurement with electron microscopy by Ing. Zdenko Gardian, Ph.D. in the Laboratory of Electron Microscopy.

I am also grateful to Barbora and Šárka from the lab for their help, creating a friendly environment, and support not only in the professional sphere.

Finally, I would like to thank my family for their loving never-ending support and patience.

Table of contents

List of abbreviations

Ab1 – primary antibodies

Ab2 – secondary antibodies

AMP – ampicillin

APS – ammonium persulfate

bp – base pair

CAN – kanamycin

CV – column volume

ddH2O – double-distilled water

dNTP – deoxynucleoside triphosphate

DLS – dynamic light scattering

Dps – DNA binding protein

EDTA – ethylenediaminetetraacetic acid

HeLp – hemo-lipo-glycoprotein

IgG – immunoglobulin G

IPTG – isopropyl β-D-1-thiogalactopyranoside

kb – kilobase

kDa – kilodalton

LB – lysogeny broth

OD600 – optical density measured at 600 nm

PAGE – polyacrylamide gel electrophoresis

PBS – phosphate-buffered saline

PCR – polymerase chain reaction

PDB – protein databank

PVDF - polyvinylidene difluoride

rpm – revolutions per minute

rSAP – shrimp alkaline phosphatase

TAE – Tris-acetate-EDTA

SOC – super optimal broth with catabolite repression

SDS – sodium dodecyl sulfate

TBDs – tick-borne diseases

TBS – Tris-buffered saline

TBEV – tick-borne encephalitis virus

TBVs – tick-borne viruses

TEMED – tetramethylethylenediamine

UV – ultraviolet

1 Introduction

1.1 Ticks

Ticks are obligate hematophagous arthropod vectors [1; 2], they are capable of transmitting viruses, bacteria and spirochetes, fungi, protozoa, or helminth parasites [1]. Concerning human and animal health, ticks are considered to be the most problematic group of exoparasites for human and animal health, right after mosquitoes [2]. Ticks transmit a variety of pathogens to the humans such as Lyme borreliosis, human granulocytic anaplasmosis, tularaemia or spotted fever rickettsiosis etc. [3].

So far, roughly 900 tick's species have been identified worldwide, and two major families of ticks are known, *Ixodidae* (hard ticks, 714 species) and *Argasidae* (soft ticks, 185 species). The third family called *Nuttalliellidae* is rarely found in southern Africa, and it is represented by only one species [4; 5]. *Ixodidae* and *Argasidae* differ in several biological aspects. Family *Ixodidae* has a teardrop body shape with a hard dorsal shield and visible gnathosoma (mouthpart including chelicerae and palps). This shield together with smooth and folded integument affects the volume of blood that *Ixodidae* can ingest. On the contrary, *Argasidae*, or soft ticks, are species without this dorsal structure and visible gnathosoma. Missing shied and leathery cuticle allows restricted yet fast expansion [5; 6]. Morphological differences between two families are shown in Figure 1. Another difference between these two families is the feeding period. Hard ticks feeding is a slow and complex process lasting for a couple of days on only one host per each life stage, unlike soft ticks for which the

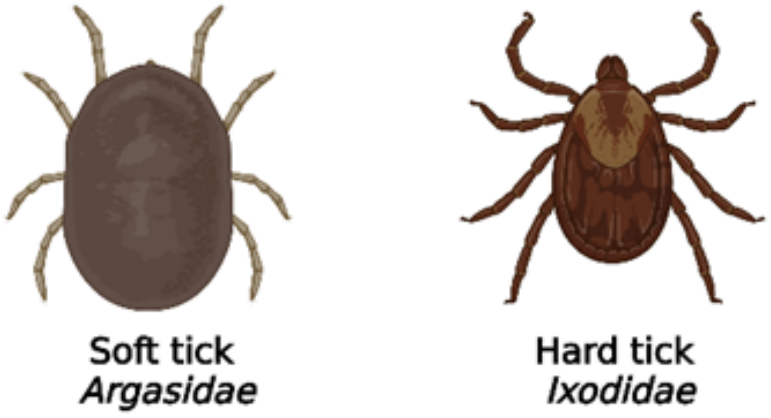

Figure 1: **Differences in morphology between Argasidae and Ixodidae** created with BioRender.com.

feeding takes less than an hour and they can change host during the nymphal and adult stages [1; 6].

1.1.1 Transmitted diseases

Ticks are known to infest a variety of hosts, including people, livestock, pets, and wildlife [7]. The majority of the diseases linked to the infection agents (bacteria, viruses and parasites) are zoonoses, for which human serves as unintentional hosts and final destination. Transmission of pathogens is mostly done by tick bites, but the host can gen infected also by alternative routes such as exposure to fluids or blood transfusions [8]. Even when ticks are not carrying tick-borne diseases (TBDs), they can cause a burden to the host by harming skin and hide, inducing allergy, irritability, and toxicosis or can reduce cattle production causing anemia [9].

Depending on the diseases, the pathogens can be disseminated within during horizontal (from tick to tick via the host), vertical (from females to eggs) or transstadial transmission (from stage to stage) [10]. Various tick species´ ability to spread disease is influenced by the length of time they spend on their host. Number of diseases transmitted by *Argasidae* is lower than by *Ixodiade.* Some species of *Argasidae* are the primary vectors for arboviral and microbial diseases, such as those caused by genus *Borrelia* [11].

Borrelia genus belongs to the *Spirochaetaceae* family, which has a spiral-shaped extracellular spirochete. Transmitted *Borrelia* genus is different for soft ticks and hard ticks, soft ticks are responsible for transmitting *Borrelia* causing relapsing fever and hard ticks transmitted genus causes *Lyme borreliosis* [12]. Zoonotic tick-borne disease *Lyme borreliosis* is one the most serious and mortal illness transmitted to humans and it is connected with encephalitis and haemorrhagic fevers [2]. The most common symptom in humans is erythema migrans, cutaneous inflammation. Depending on the infectious agent, the lesion may cause cardiac, joint, neurological, or cutaneous disorders in the absence of antibiotic therapy [12].

Tick-borne viruses (TBVs), commonly referred to as tibo viruses, are a group of various viruses that effectively spread across two different environments [13]. The majority of these viruses are members of Bunyaviridae, Flaviviridae, and Reoviridae families [14]. One of the most viral tick-borne illnesses in humans is tick-borne encephalitis, which is caused by the tick-borne encephalitis virus (TBEV). TBEV belongs to RNA viruses, and it

is transmitted to the ticks during feeding on a vertebrate host at the viremic phase. Virus is then transmitted to the new host during the next feeding [10]. After infection, the first symptoms are similar to influenza-like illness, after this stage, a short time of improvement appears, and meningitis or myelitis symptoms may be eventually manifestated [15].

1.2 *Ixodes ricinus*

The common usual tick species from the *Ixodidae* family in Europe is *Ixodes ricinus*. This species is widespread mainly due to its reproduction rate, broad host range and ability to withstand most environmental conditions [16].

Ixodes ricinus developmental stages, presented in Figure 2, include egg, larva, nymph, and adult form [17]. Except for the egg stage, all the life stages parasitize on a single host for a couple of days. Host´s blood serves as a unique nutrition source for their development, reproduction, egg and sperm production [6; 18]. Altogether the feeding duration lasts about 12-20 days. All active developmental stages stay attached to the host while imbibing blood for several days – larvae for 2-4 days, nymphs for 4-6 days and adult females spend 6-10 days [19]. After feeding, larvae and nymphs moult and transform into the next stage

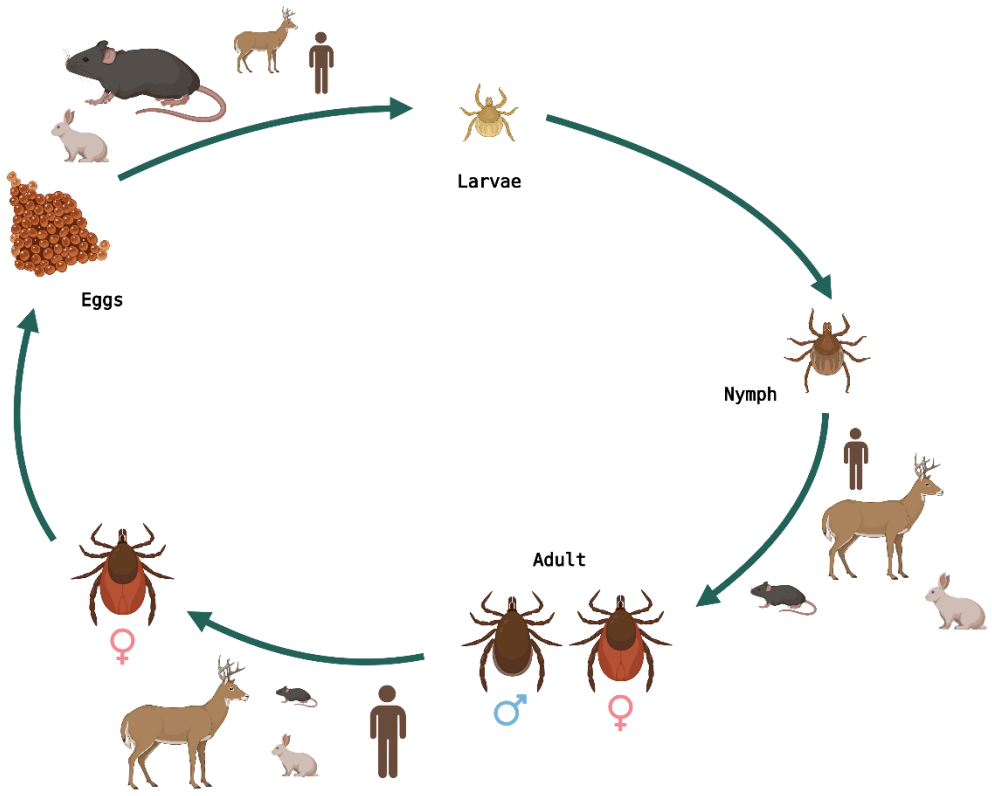

Figure 2: **Life cycle of *Ixodes ricinus***: The size of the host represents preferable type of the host in a different stage of tick (created with BioRender.com). Male ticks fertilize an adult female. Female ticks lay eggs after feeding on "reproduction" host and then subsequently die [19].

(shed the cuticle), while the adult female lays a single clutch of eggs and dies [17]. In nature, the life cycle of *Ixodes ricinus* lasts between two to six years. For finding a new host, ticks climb on the grass to get close to the host. Their sensory system – Haller´s organ is sensitive to vibration, odour, or temperature changes. This sensory system, located on each tarsus of the first pair of legs, helps ticks to find suitable hosts [6].

Iron is an essential element for most organisms and works as an electron donor/acceptor in different metabolic processes, but a high level of free iron created a burden for the organism [20]. Ferritin, transferrin or heme oxygenase are iron-binding proteins that regulate iron levels in the cells and prevent possible toxicity of iron in higher concentrations [21]. Heme oxygenase controls heme catabolism in vertebrates, and toxic ferric ions are transported via transferrin, which also keeps iron in the non-toxic way (bioavailable form). In the majority of organisms, ferritin serves as a cytosolic storage protein for iron [22].

1.3 The Ferritin Superfamily

The Ferritin Superfamily consists of about 11,500 members, divided into three sub-families [23; 24; 25]:

1) the classical ferritins (the most abundant group)
2) the bacterioferritins
3) the Dps proteins (DNA binding protein from starved cells).

Structural pattern for the Ferritin Superfamily is the four α-helix bundle structure. Examples of the members of the superfamily are ferritins, soluble methane monooxygenases, ribonucleotide reductases, rubrerythrins, Dps-like proteins, or archaeoferritins [26; 27]. Ferritins and bacterioferritins have many structural and functional similarities, their shared main function is to store the iron. However, the Dps proteins play a role in iron detoxification [28]. There are large differences in structures between ferritins, bacterioferritins and Dps protein, especially in primary and quaternary structures. Dps and Dps-like quaternary structure is made from 12 subunits, while ferritins and bacterioferritins consist of 24 identical subunits [29].

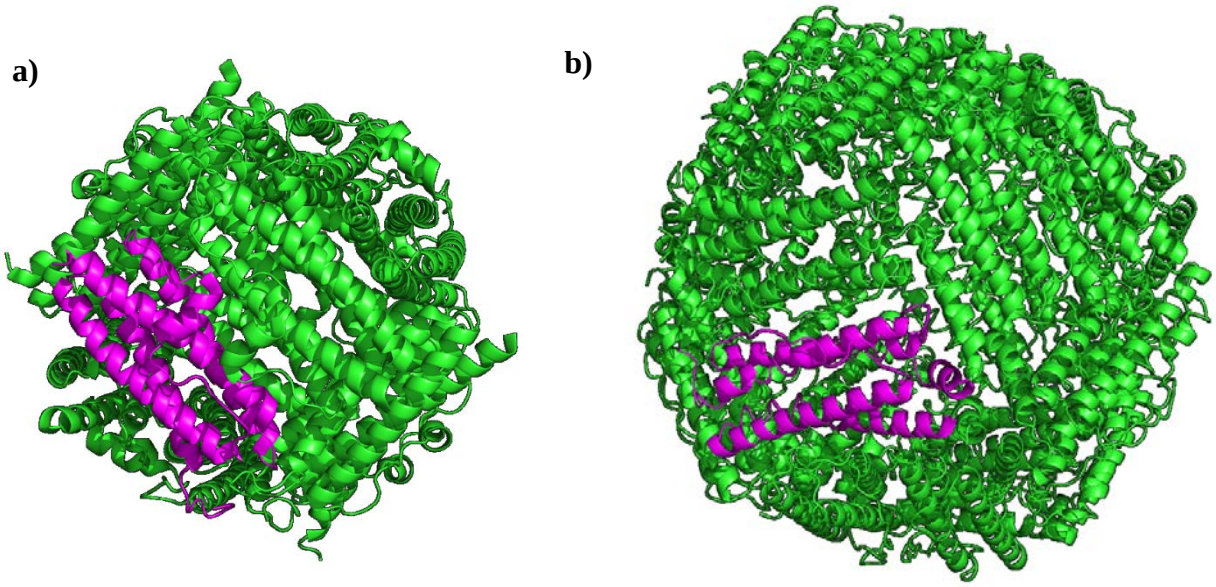

Figure 3: **Structures of Dsp protein and ferritin with highlighted subunit (magenta): a)** X-ray structure of Dps protein from *Thermosynechococcus elongatus* (PDB code: 2C41) with 12 subunits. **b)** X-ray structure of the whole recombinant ferritin from mouse (right, PDB code: 1LB3) with 24 subunits. Both are visualised by PyMOL.

Structurally similar ferritins and bacterioferritis form a sub-family - the Ferritin-like superfamily. All members of the sub-family are capable of storing iron [30]. Ferritins are found in the majority of organisms – humans, invertebrates, plants, or microorganisms [31]. The ferritin-like superfamily structure pattern is represented by 24 subunits, where each subunit consists of four tightly packed α-helices (A-D), a loop that connects two of the helices (B-C), and a short fifth α-helix (E) [32]. The 24 subunits only fold after the construction of a stable dimer. This shows that there is a twofold symmetry, due to the loop between two helixes (B-C) in one subunit with the same loop in another subunit [33]. Ferritin´s structure is composed of a heavy chain (ferroxidase site) and a light chain (nucleation site) [34]. In the ferritin structure, there are six C_4 channels, which allow the entrance of Fe(II) or water into the structure, and eight C_3 channels permit the entry of O_2 or small organic molecules [35].

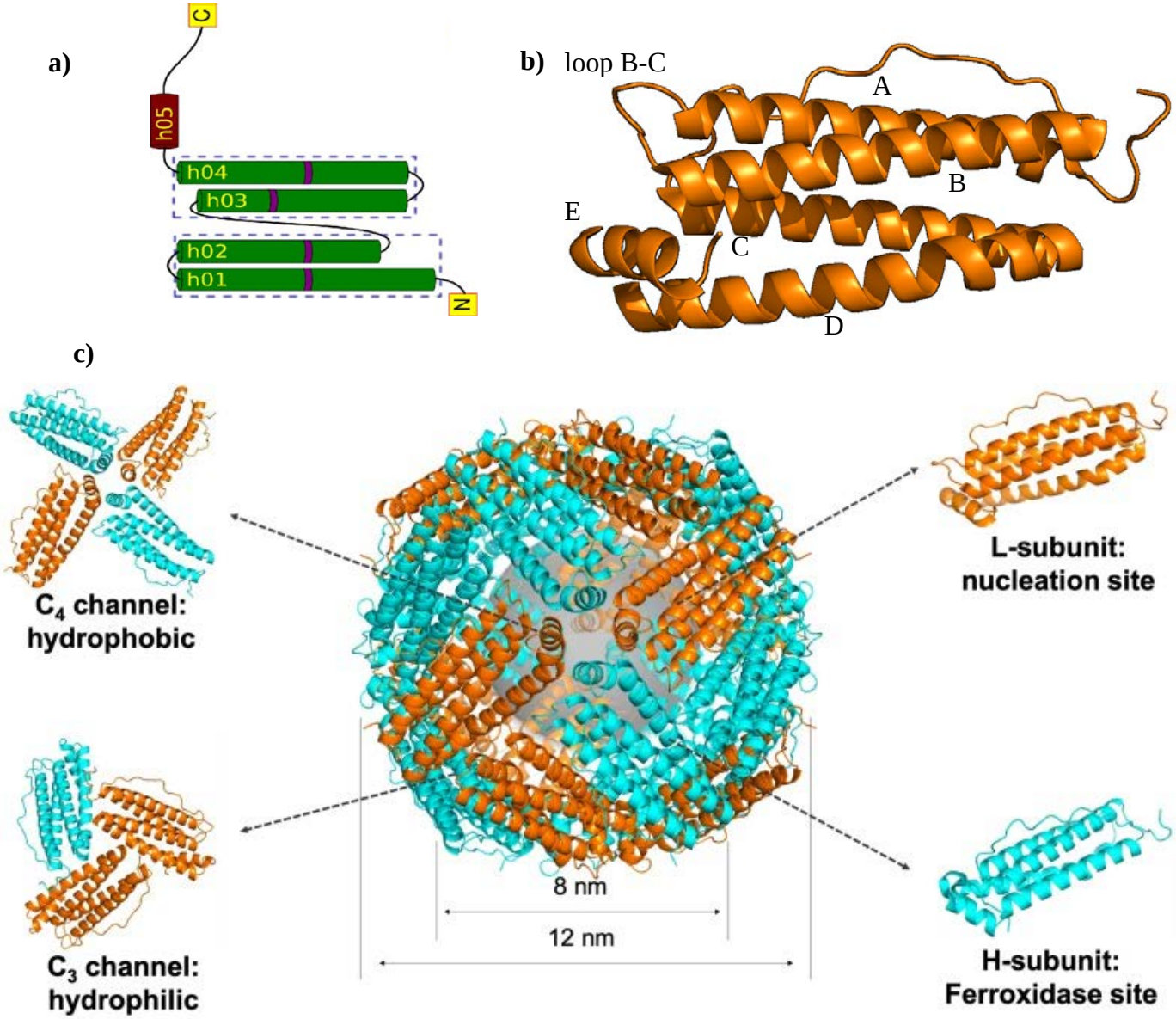

Figure 4: **The ferritin fold (a):** In the model, there is a characteristic four-helix bundle, four helixes in the complex are in an up-down-down-up topology. Complex coordinates a pair of metal ions. The location of residues that are connected to the iron is purple [55]. **Structure of one subunit (b):** Model of one subunit of ferritin from mouse (PDB code: 1LB3) obtained by X-ray diffraction visualized by PyMOL. The subunit consists of four long α-helixes, one short α-helix and a random coil for connection to another subunit [56]. **X-ray structure of whole recombinant ferritin (c):** Model from human heavy chain ferritin (PDB code: 5N27) obtained by X-ray diffraction with highlighted nucleation/ferroxidase site and C_4 channel with hydrophobic property and C_3 channel with hydrophilic function. Inner diameter of ferritin is 8 nm, while outer diameter is 12 nm. Adapted from [57].

There are large differences in primary structures from different species, while the secondary, tertiary, and quaternary structures remain very similar [35]. Structures of ferritins from different species were determined by X-ray crystallography, including species such as human (PDB code: 1FHA) [36], horse (PDB code: 1IER) [37], frog (PDB code: 1MFR) [38], insect (PDB code: 1Z6O) [39], soybean (PDB code: 3A9Q) [40], or *E. coli* (PDB code: 1EUM) [41].

Ferritins regulate iron homeostasis by storing and releasing iron, each step is controlled to avoid the toxicity of iron [25]. The toxicity of iron is caused by harmful redox reactions, which could damage proteins, lipids, or DNA. By preventing these reactions, the protein coat helps iron core maintain its solubility [23]. The shape of the structure of ferritins is critical to their function. Each identical subunit performs a building block for the assembly of protein and storage iron [42]. Accumulation of iron is possible due to the hollow centre acting as a large cavity [32]. The two Fe(III) ions are coordinated to Glu23, and Glu58 at site A and to Glu58 and Glu103 at side B [43]. Due to the chemical reduction of Fe(III) to Fe(II), iron is released from ferritin. After reduction, iron creates a complex with chelating agent – bipyridyl [44; 45] or flavoproteins [46].

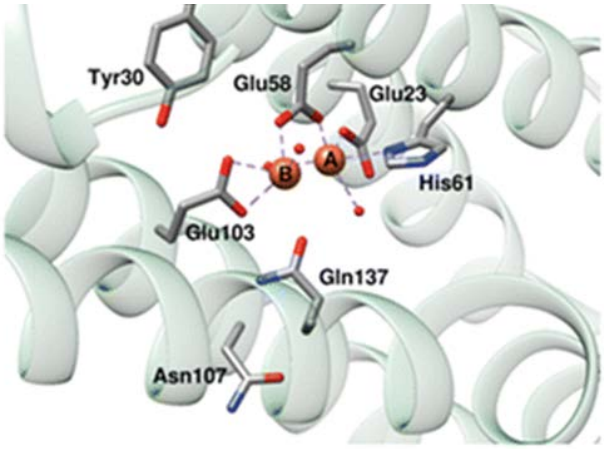

Figure 5: **Ferroxidase centre of ferritin:** Ferroxidase centre is shown on the model of ferritin from bullfrog (PDB code: 3RCB) [58].

1.4 Ferritins in ticks

Two types of ferritin – I and II, with different functions can be found in ticks [47]. Ferritin´s I function is known, it is intracellular storage, capable of storing up to 4 500 iron atoms. On the other hand, the function of ferritin II is not clearly known, but it probably plays a crucial role in the transport of non-heme iron. The tick´s gut produces ferritin II, which is then released into the haemolymph [47]. Each ferritin subunit has approximately 21-25 kDa, in total circa 500-600 kDa [48].

Ticks suck enormous amounts of iron in blood during feeding. Ticks gain iron from the host in two different ways:

- heme in hemoglobin in red blood cells
- iron in host serum iron-containing proteins such as ferritin or transferrin.

The fates of these two substances, shown in Figure 6, differs in tick organism. During digestion in the lysosome, heme is released from hemoglobin. The heme is transported into peripheral tissue cells or detoxified by aggregation and storage in hemosomes [47; 49]. Transport is mediated by HeLp protein (heme-binding lipoprotein), whose main goal is to fulfil cell heme requirements. Iron, from the host serum containing iron proteins, is released from the endosome into the cytoplasm, and then it could be captured by ferritin I or loaded into ferritin II. To meet the cell iron requirements, iron captured by ferritin II is transported from the endosome via hemolymph into peripheral tissues [47].

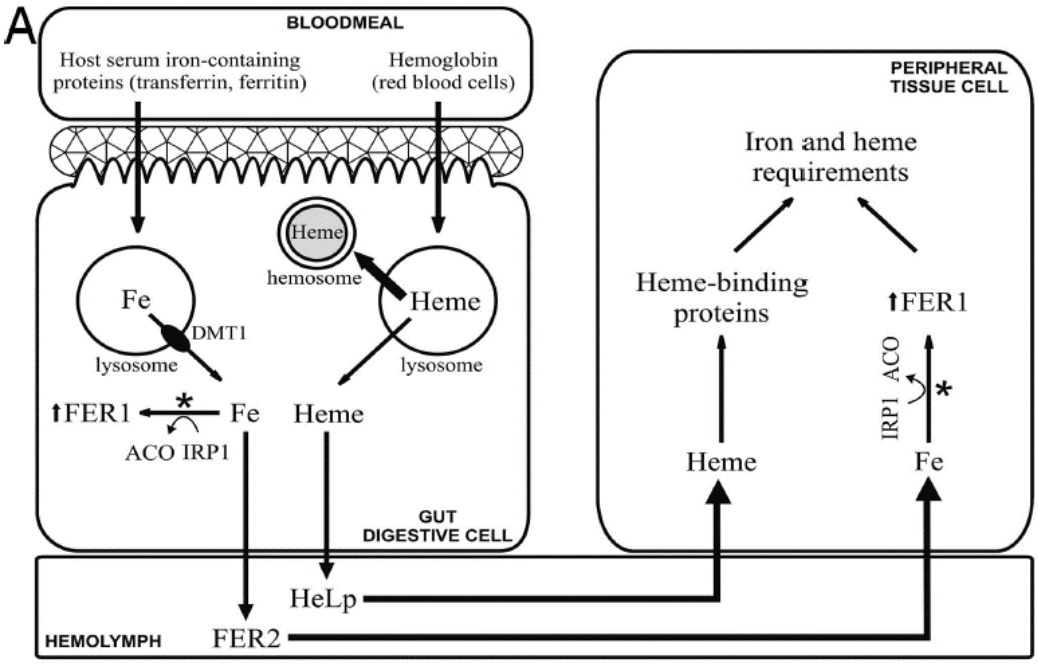

Figure 6: **Fate of heme and iron in tick´s digestive system:** individual ways of heme and iron from gut digestive cell to peripheral tissue cell [47].

Both ferritins have unique roles in blood feeding and egg development; especially ferritin II has a detrimental effect on tick development and reproduction. Ferritin II is produced during all tick stages. Depletion of ferritin II during RNA interference showed up that expression of ferritin I stops in the salivary glands. In contrast, the amount of ferritin II is not affected by the silencing of ferritin I. This means that ferritin II is not regulated by ferritin I. Complete knockdown of ferritin II results in the loss of the tick´s ability to feed, this results in the drying of ticks on the host in a short time after the attachment and ends with dropping off of the ticks. It shows that ferritin II has a crucial role in blood indigestion [47].

These findings show that ferritin II is a promising candidate for an effective anti-tick vaccine. Vaccine against tick proteins possibly reduces the risk of transmitting pathogens from *Ixodes ricinus.* During the vaccination experiments, infested rabbits vaccinated with recombinant ferritin II had a lower chance of tick infestation. Vaccine efficacy is high which results in reducing the number of ticks, and overall ticks started to lose weight and the ability to reproduce [47; 50].

1.5 Aims of the thesis

The aims of this master thesis were:

1. Prepare soluble recombinant ferritin II from *Ixodes ricinus* with and without His-tag
2. Purify recombinant ferritin II, verify refolding from inclusion bodies and proper folding
3. Prepare a sample for CryoEM

2 Materials and methods

All used solutions with their composition are listed in Chapter 8 Supplements.

2.1 Primer design

The construct of ferritin II in pET100/D-TOPO (Invitrogen) vector was obtained from the Laboratory of Molecular Biology of Ticks, Institute of Parasitology and used as template for PCR. Ferritin II was amplified using primers in Table 1 and cloned into four different cloning vectors (Table 2) using either restriction enzymes or Nebuilder cloning kit (NEB). Alle primers were designed manually or using NEBuilder Assembly Tool (http://nebuilder.neb.com/#!/). The absence of cleavage specific site of used restriction enzymes within ferritin II, the gene was verified by NEBCutter restriction tool from BioLabs New England (https://nc3.neb.com/NEBcutter/).

Table 1: Primer design for amplification of the fragments

Vector	Primer	Sequence (5'-3')	Length [bp]	GC content [%]	Restriction enzyme
pASK-IBA37+	Fer2-pASK37-F	ATGGTAGGTCTCAGCGCGGGAACAATTTGTTCGAAAACCTG	24	41.7	BsaI
	Fer2-pASK37-R	ATGGTAGGTCTCATATCAAAATTC CTTCTTGTCTCCGAGCA	23	43.5	
pETSUMO	Fer2-SUMO-F	CACAGAGAACAGATTGGTGGAGGGAACAATTTGTTCGAAAACCTG	24	-	-
	Fer2-SUMO-R	TGTCTCCTGAGTTCTAGAGTACTTTAAAATTCCTTCTTGTCTCCGAGCA	23	-	-
pET21d	Fer2-pET21d-F	ATGGTAGGATCCATGGGGAACAAT TTGTTCGAAAACCTG	24	41.7	BamH1
	Fer2-pET21d-R	ATGGTACTCGAGTCAAAATTCCTTCTTGTCTCCGAGCA	23	43.5	Xho1
pASK-IBA33+*	Fer2-pASK33-F	ATGGTAGGTCTCAGCGCATGGGGAACAATTTGTTCGAAAACCTG	24	41.7	BsaI

*Reverse prime – Fer2-pASK37-R

Table 2: Specification of vectors

Vector	His-Tag	Cloning	Antibiotic resistance
pET100	✓	restriction digestion	ampicillin
pASK-IBA37+	✓	restriction digestion	ampicillin
pETSUMO	✓	Nebuilder cloning kit	kanamycin
pET21d	x	restriction digestion	ampicillin
pASK-IBA33+	x	restriction digestion	ampicillin

2.2 Gradient PCR

For optimization of annealing temperature of each primer, gradient PCR was done with increasing temperature using PPP MasterMix (TopBio) according to the manual. Reaction mixes were made according to the Table 3 and PCR was performed in Biometra Tone Thermal Cycler (Analytik Jena). Amplification program is recorded in Table 4.

Table 3: Gradient PCR - composition

Reagent	Volume [µl]
PPP MasterMix	12.5
Forward primer	1
Reverse primer	1
PCR H_2O	9.5
Template DNA	1
Total volume	25

Table 4: Gradient PCR - amplification program

Stage	Temperature [°C]	Time	
Initial denaturation	94	1 min	
Denaturation	94	15 sec	30x cycles
Primer annealing	54,0-54,3-54,9-55,9-57,4-59,3	15 sec	
Elongation	72	1 min/kb	
Extension	72	7 min	
Cool down	16	∞	

Amplicons were separated by agarose gel (1% agarose in 1x TAE) and stained with Serva DNA Stain Clear G (SERVA Electrophoresis). 100 bp DNA Ladder (New England Biolabs) was also loaded. Loaded samples were run at 100 V, 400 mA for 30 minutes and the gel was visualised in G:BOX Chemi-XX6 (SynGene).

2.3 Q5 PCR

For amplification of DNA fragments, Q5® High-Fidelity DNA Polymerase (New England Biolabs) was used. Preparation of the mixture for Q5 PCR is written in Table 5 and the Q5 PCR program is in Table 6. Briefly, the Q5 PCR started with initial denaturation for 30 sec at 98 °C, followed by repeated steps – denaturation, primer annealing and elongation. Temperature for primer annealing was selected from gradient PCR results.

Table 5: Q5 PCR - composition

Reagent	**Volume [µl]**
5x Q5 reaction buffer	10
10 mM dNTPs	1
10 µM forward primer	2.5
10 µM reverse primer	2.5
Template DNA	1
Q5 High-Fidelity DNA Polymerase	0.5
5x Q5 High GC Enhancer (optional)	(10)
PCR H_2O	32.5(22.5)
Total volume	50

Table 6: Q5 PCR - amplification program

Stage	**Temperature [°C]**	**Time**	
Initial denaturation	98	30 sec	
Denaturation	98	15 sec	35x cycles
Primer annealing	Selected	30 sec	
Elongation	72	20 sec/kb	
Extension	72	2 min	
Cool down	10	∞	

Samples were separated on 1% agarose gel as described in Chapter 2.2 Gradient PCR and corresponding DNA amplicons were cut out from the gel and purified with NucleoSpin® Gel and PCR Clean-Up kit (Macherey-Nagel), following the extraction manual from the producer. NanoDrop one (Thermo Scientific) was used to measure the DNA concentration.

2.4 Cloning of DNA

Conventional cloning using restriction enzymes NEBuilder® HiFi DNA Assembly (New England Biolabs) was used to clone ferritin II amplicon into individual expression vectors.

2.4.1 NEBuilder® HiFi DNA Assembly

The assembly was done according to the manual from New England Biolabs in a 1:2 vector to insert molar ratio (Table 7). Amplified ferritin II was mixed with pETSUMO vector and then 5 µl of HiFi Mater Mix was added to the mixture. The mixture was incubated at 50 °C for 30 minutes and then put on ice before being transformed.

Table 7: NEBuilder cloning - composition

Reagent	Amount
Vector pETSUMO	0.04 pmol
Insert ferritin II	0.08 pmol
HiFi Master Mix	5 µl
PCR H_2O	Up to 10 µl

2.4.2 Restriction digestion

BsaI restriction enzyme was used for restriction digestion in order to accomplish cloning into pASK-IBA37+ and pASK-IBA33+, for cloning into pET21d BamHI and XhoI restriction enzymes were used instead. Digestion of DNA fragments and cloning vectors was done according to Table 8, the mixture was incubated at 37 °C for 15 minutes, followed with enzyme deactivation at 65 °C for 20 minutes. For dephosphorylation of vectors, 2.5 µl of Shrimp alkaline phosphatase (rSAP) was added to the vector reactions and the mixture was incubated for another 30 minutes at 37 °C and deactivated for 5 minutes at 65 °C. All digested products were purified using NucleoSpin® Gel and PCR Clean-Up (Macherey-Nagel) following the PCR clean-up protocol.

Table 8: Set up of the digestion reaction

Reagent	Amount	
	DNA - insert	DNA - vector
DNA	1 µg	1 µg
10x CutSmart Buffer	5 µl	5 µl
Restriction enzyme(s)	1 µl	1 µl
PCR H_2O	Up to 50 µl	Up to 50 µl

T4 DNA ligase (Invitrogen) was used for ligation of the digested fragments and corresponding vectors together in a 3:1 insert to vector molar ratio. The exact composition of ligation reaction is stated in Table 9. The reaction was incubated at 16 °C overnight and then deactivated for 10 minutes at 65 °C followed by transformation.

Table 9: Ligation - composition

Reagent	Amount
Vector	0.02 pmol
Insert ferritin II	0.06 pmol
10x T4 DNA ligase buffer	2 µl
T4 DNA ligase	1 µl
PCR H_2O	Up to 20 µl

2.5 Transformation of *E. coli* competent cells

Heat shock transformation was made into several different competent *E. coli* cells, such as NEB® 5-alpha(High Efficiency) (New England Biolabs), BL21-CodonPlus(DE3)-RIPL (Agilent Technologies), Rosetta™(DE3) (Novagen), BL21(DE3) (New England Biolabs), ArticExpress(DE3) (Agilent Technologies). Transformation of each competent cell is almost similar; the difference is in the time of heat shock listed in Table 10. Transformation with NEB® 5-alpha cells was done with ligation reaction followed by colony PCR and isolation of plasmid. The rest of the cells were used for protein expression with plasmid DNA.

Table 10: Duration of heat shock for individual *E. coli* strain

***E. coli* competent cells**	**Heat shock [s]**
NEB® 5-alpha	30
BL21-CodonPlus	20
Rosetta™	30
BL21(DE3)	10
ArticExpress	20

First, a tube of competent cells was thawed on the ice for 20 minutes, and then the appropriate volume of ligation mixture (concentration 5 ng) or plasmid DNA (concentration 1 pg-100 ng) was added. The mixture in tube was carefully flicked 4-5 times and incubated on the ice for 30 minutes.

Heat shock was performed at 42°C for defined time in a water bath. Subsequently, the mixture was incubated for 5 minutes on ice. To the mixture 250 µl prewarmed SOC medium was added and the mixture was placed for an hour in an Eppendorf Innova® S44i horizontal shaker, preheated at 37°C at 250 rpm. Meanwhile, LB plates with specific antibiotics for appropriate plasmid were incubated at 37°C. Antibiotic resistances for each vector are written in Table 2. In the case of BL21-CodonPlus cells, chloramphenicol was also presented on the plates. After shaking, 50 µl of the mixture was spread on one plate and the rest on the second plate. Plates were put in the incubator at 37°C overnight.

2.6 Colony PCR-Same protocol as for Gradient PCR

Twelve single colonies, which were obtained from the transformation of ligation reaction into NEB® 5-alpha competent cells, were picked up with a pipette tip and put into 20 µl of PCR H_2O. With a pipette tip, a cross was made on pre-warmed LB plates with specific antibiotics. Verification of the presence of the ferritin II gene was done by colony PCR. Composition of the master mix for the PCR reaction was the same as for gradient PCR (TopBio PPP Master Mix protocol) according to Table 3. The 1 µl of PCR H_2O with the single colony was used as template DNA. Negative control was picked out from plates without single colony. Amplification program was also the same except for the time of initial denaturation, which lasted for 6 minutes. Identification of positive colonies was visualized on 1% agarose gel in G:BOX Chemi-XX6 (SynGene).

2.7 Plasmid isolation

Positive colonies were inoculated into the 15-ml cultivation tubes together with 4 ml of LB medium and specific antibiotics (Table 2). Tubes with the mixture were incubated overnight at 37°C in Eppendorf Innova® S44i horizontal shaker. The following day, plasmids, harvested by centrifugation at 11 000 x g for 30 sec, were isolated using Nucleo-Spin® Plasmid (NoLid) kit (Macherey-Nagel) following High-copy plasmid DNA from *E. coli* protocol. Plasmid DNA was eluted with 50 µl of PCR H_2O and the concentration was measured with NanoPhotometer® Pearl (Implen). Selected samples were sent to SEQme company for Sanger sequencing.

According to the results from sequencing, verified colonies carrying the desired plasmid were selected for maxiprep. From colony PCR cross cells were picked up and put into 150 ml of LB medium with specific antibiotics. Mixtures were incubated overnight at 37°C in Eppendorf Innova® S44i horizontal shaker. After harvesting of bacterial cells by centrifugation at 5000 x g, at 4 °C for 10 minutes, the plasmid was isolated by protocol High-copy plasmid purification using Nucleobond® Xtra Midi kit (Macherey-Nagel). Concentration of purified plasmid was measured with with NanoPhotometer® Pearl (Implen).

2.8 Pilot expression

Ferritin II protein production was tested in various expression cells including *E. coli* BL21-CodonPlus(DE3)-RIPL (Agilent Technologies), Rosetta™(DE3) (Novagen), ArticExpress(DE3) (Agilent Technologies). The effect of temperature, time of expression or concentration of inducer was evaluated.

From plates with the appropriate plasmid, one grown colony was picked up using a yellow tip and placed into 10 ml of LB medium with a selective antibiotic in concentration of 100 µg/ml. In the case of ArticExpress(DE3) cells, gentamycin was added to the mixture in concentration of 20 µg/ml and for BL21codon+ chloramphenicol was added in concentration of 100 µg/ml. Cells were incubated overnight at 37 °C, 220 rpm in Eppendorf Innova® S44i horizontal shaker. The following day, 1 ml of overnight culture was added to the 15 ml of LB medium with corresponding antibiotics, no antibiotics were added to the expression in ArcticExpress cells.

Within the exception of ArcticExpression(DE3) cells, all expression cells were incubated in Eppendorf Innova® S44i horizontal shaker at 37 °C, 220 rpm until the OD_{600} reached 0.4-0.6. Protein production was induced by IPTG (Isopropyl β-D-1-thiogalactopyranoside) at concentrations of 0.5 mM and 1 mM for pET100, pETSUMO, and pET21d vectors. The protein production for pASK-IBA33+ and pASK-IBA37+ vectors was induced by ATC (anhydrotetracycline) at concentration of 200 µg/l. Two temperatures were selected for optimization of production – 18 °C and 37 °C respectively and cells were placed in Eppendorf Innova® S44i horizontal shaker at 220 rpm. For 18 °C, 1 ml samples from each culture were taken after 3, 6 hours and overnight, for 37 °C, 1 ml samples from each culture were taken after 2, 4, and 6 hours. Collected samples were pelleted at 11 000 x g for 5 minutes and pellets were stored at -20 °C for further evaluation of protein production.

ArcticExpression(DE3) cells were incubated at 30 °C at 220 rpm in Eppendorf Innova® S44i horizontal shaker for 3 hours. Then the temperature of shaker was set to 13 °C and the production of protein was induced by either IPTG or ATC as described above. 1 ml samples were collected after 6 hours, overnight and after 24 hours, pelleted at 11 000 x g for 5 minutes and placed into the freezer at -20 °C.

2.9 SDS-PAGE electrophoresis

SDS-PAGE electrophoresis was used for evaluation of protein production and purification. Firstly, SDS-PAGE was used for evaluation of pilot expression and determination if protein produce in soluble or insoluble fractions. Cell pellets from pilot expression were resuspended in 500 µl of lysis buffer. Three cycles of freezing in liquid nitrogen and thawing at 42 °C were used to lyse the cells. Resulting cell lysate was centrifugated at 13 200 x g at 4 °C for 5 minutes to separate soluble and insoluble fractions. Supernatant was transferred into the new tube and 4x SDS-PAGE sample buffer was added. Pellets were mixed with 1x SDS-PAGE sample buffer. All samples were boiled at 95 °C for 5 minutes and analysed on 15% SDS-PAGE gel (Table 11). PageRulerTM Protein Prestained Ladder or PageRuler™ Unstained Protein Ladder (Thermo Fischer Scientific) were used as molecular standards. Electrophoresis was done in 1xSDS-PAGE running buffer. After the samples were loaded on the gel, SDS-PAGE ran for 30 minutes at 100 V and then for 1 hour at 150 V. Next the gel was transferred into 20 ml of fixing solution for 30 minutes, followed by two washes in ddH_2O for 10 minutes on rocking platform. Finally, the gel was left

overnight in 20 ml of staining solution. Gel pictures were made with G:BOX Chemi-XX6 (Syngene).

Table 11: Preparation of eight 15% gels for SDS-PAGE

Reagent	15% separation gel		5% stacking gel	
	30% acrylamide	40% acrylamide	30% acrylamide	40% acrylamide
Acrylamide	20 ml	15 ml	2.67 ml	2 ml
ddH_2O	9.16 ml	14.16 ml	11 ml	11.66 ml
1.5M Tris pH 8.8	10 ml	10 ml	-	-
1M Tris pH 6.8	-	-	2 ml	2 ml
10% SDS	400 µl	400 µl	160 µl	160 µl
10% APS	400 µl	400 µl	160 µl	160 µl
TEMED	40 µl	40 µl	16 µl	16 µl

2.10 Western blot

In some cases, for verification of protein presence western blot was made after SDS-PAGE. An Immun-Blot® PVDF membrane (Biorad) was equilibrated in 100 % methanol for 15 minutes on a rocking platform followed by 15 minutes in 1x Transfer buffer. The gel from SDS-PAGE electrophoresis was equilibrated in 1x Transfer buffer for 15 minutes on a rocking platform. The blotting sandwich was assembled according to Figure 7 and placed in a cassette of Trans-Blot® Turbo (Biorad). The whole sandwich was wetted in the 1x Transfer buffer. After the assembly, the sandwich was de-bubbled using a blot roller and the transfer was run at 25 V, 1A for 30 minutes. The membrane was taken out of the blotting sandwich and washed three times for 10 minutes in 1x TBS-T. Meanwhile, 5% blotting-grade non-fat dry milk (Biorad) was prepared in 1x TBS-T. The membrane was incubated in 5 % blocking solution for 1 hour on a rocking platform and washed three times for 10 minutes in 1x TBS-T. Next, the membrane was incubated with the primary antibody (Ab1, Table 12) in 5% blocking solution overnight at 4 °C.

Table 12: Specification of used antibodies for each vector

Vector	Ab1	Ab1:TBS-T	Ab2	Ab2:TBS-T
pASK-IBA37+	mouse primary Monoclonal anti-polyhistidine antibody (Sigma, H1029)	1:3 000	goat Anti-mouse IgG-peroxidase antibody (Sigma, A5278)	1:5 000
pETSUMO	mouse primary Monoclonal anti-polyhistidine antibody (Sigma, H1029)	1:3 000	goat Anti-mouse IgG-peroxidase antibody (Sigma, A5278)	1:5 000
pET21d	rabbit antibodies	1:500	Anti-Rabbit IgG-Peroxidase antibody from goat (Sigma Aldrich, A9169)	1:100 000
pASK-IBA33+	rabbit antibodies	1:500	Anti-Rabbit IgG-Peroxidase antibody from goat (Sigma Aldrich, A9169)	1:100 000

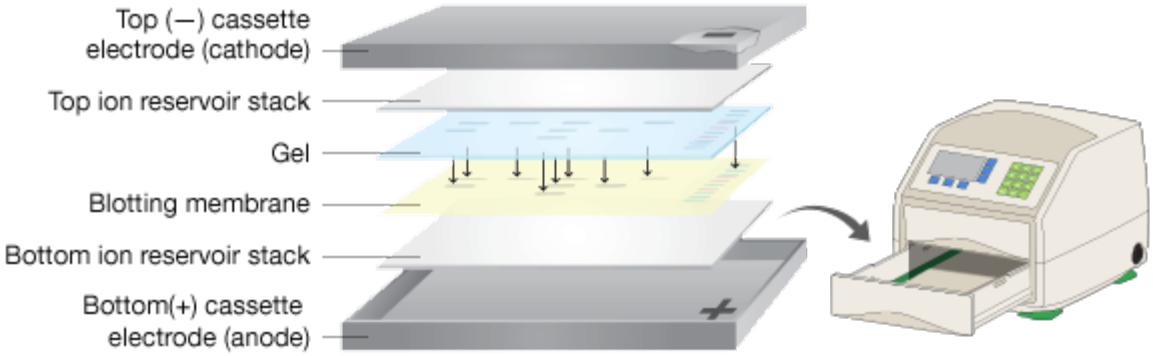

Figure 7: **Western blot sandwich composition** from the brochure from the producer Biorad

Next day, the membrane was washed two times in the 1x TBS-T for 10 minutes and then one time in the 1x TBS for 10 minutes. Secondary antibodies (Ab2, Table 12) were added to the membrane and incubated for 1 hour on a rocking platform. Finally, the membrane was washed three times in 1x TBS for 10 minutes. Signal development was done using Clarity® Western ECL Substrate (Biorad), and the components were mixed in a 1:1 ratio. The membrane was incubated in the mixture for 5 minutes and then photographed with G:BOX Chemi-XX6 (Syngene).

2.11 Large-scale expression

According to the results from pilot expression of each plasmid, conditions for large scale expression were selected. Large scale expression was done in

BL21-CodonPlus(DE3)-RIPL, BL21(DE3), and ArticExpress(DE3) cells. Overnight culture was inoculated the same way as during pilot expression.

Overnight cultures were transferred to 800 ml of new LB medium and incubated in an Eppendorf Innova® S44i horizontal shaker at 37°C, 220 rpm until value of the OD_{600} reached 0.6-0.8. According to the used plasmid, the inducer was picked and used for stimulation of protein production. Cells with plasmid were then incubated at selected temperatures and times by results from pilot expression. In the end, centrifugation was used for harvesting the cells at 4 °C, 4 000 rpm for 30 minutes. The cell pellet was stored at -80 °C for later use.

In order to optimize protein production, extra steps were added to the large-scale expression protocol. One optimization was done with the glucose step when the transformation and overnight culture were done the same way as written before. Overnight culture was transferred into 400 ml of fresh LB with appropriate antibiotics and 1 M sterile filtered glucose was added to the final volume of 20 mM. Culture was incubated at 30 °C for 4-6 hours until OD_{600} reached 1.5, followed by spinning at 3000 x g for 10 minutes. Supernatant was removed and 800 ml of fresh LB medium was used for resuspending the pellet. Adding an inducer, culture was grown at 30 °C, 180 rpm overnight. The following day, cells were collected by centrifugation at 3000 x g for 10 minutes.

Supplementation with iron was used to support protein production. With a specific inducer, iron in concentration 5 mg/l was added to the 800 ml LB medium with overnight culture and selected antibiotic. Culture was incubated at 30 °C, 180 rpm overnight and then harvested at 4 °C, 4 000 rpm for 30 minutes.

2.12 Isolation of inclusion bodies

Two ways were used for isolation of inclusion bodies – sonication protocol and microflow. All samples from each step of isolation were analysed by SDS-PAGE electrophoresis.

2.12.1 Sonication protocol

In the sonication protocol of isolation of inclusion bodies were used three buffers:

- Buffer 1: 20 mM Tris, pH 8.0

- Buffer 2: 2M urea, 20 mM Tris-HCl, 0.5 M NaCl, 10 mM imidazole, 1 mM β-mercapthoethanol, 2% Triton X-100, pH 8.0
- Buffer 3: 6 M guanidine hydrochlorid, 20 mM Tris-HCl, 0.5 M NaCl, 5 mM imidazole, 1 mM β-mercapthoethanol, pH 8.0

Pellets from the large-scale expression were resuspended in Buffer 1 (4 ml/100 ml of original culture). On the ice, the mixture was sonicated 3-4 times for 30-60 seconds at 0.5 amplitude at 50-60% and then spined down at 4 °C, 13 000 rpm for 10 minutes. Supernatant was discarded and pellet was resuspended in Buffer 2 (3 ml/100 ml of original culture), sonicated 3 times for 60 seconds, and spined down at 4 °C, 13 000 rpm for 10 minutes. Supernatant was poured out. Resuspending step in Buffer 2, sonication and pelleting was repeated until obtaining colourless supernatant. Then, the pellet was resuspended in Buffer 3 (5 ml/100 ml of original culture). The mixture was stirred at room temperature overnight and then centrifugated at 4 °C, 13 000 rpm for 15 minutes. Supernatant was filtrated through 0.22 µm filter. For gel analysis, 100 µl of supernatant was removed and dialysed in H_2O due to the presence of guanidine hydrochlorid. Dialysis was done in distilled water in Dialysis tubing cellulose membrane (Sigma-Aldrich) tube until white precipitation appeared. To the 30 µl of the precipitated sample, 10 µl of 4x SDS-PAGE sample buffer and sample was boiled at 95 °C for 5 minutes.

2.12.2 Microflow isolation

An alternative approach of isolation of inclusion bodies was done with microflow. First, lyse of cells from large-scale expression was done using M20 Microfluidizer® Processor (Microfluidics). After being defrosted on ice, pellets from the large-scale expression were resuspended in lysis buffer (10 ml/800 ml of original culture) containing protease inhibitor (SIGMAFAST Protease Inhibitor Cocktail tablets, EDTA-free by Sigma-Aldrich), DNase I and RNase I (10 µg/mL final concentration) (PanReac AppliChem). Then, cells were lysed with Microfluidizer at 20 000 PSI and centrifugated at 4 °C, 40 000 rpm for an hour. Obtained insoluble fraction was dissolved in Buffer 3 (described above) and by stirring overnight at room temperature to solubilize inclusion bodies. Mixture was centrifugated at 4 °C, 40 000 rpm for 30 minutes and supernatant with inclusion bodies was used for denaturating purification. Sample for analysis was done the same as above.

2.13 Denaturating purification

Supernatant from isolation of inclusion bodies was used in IMAC denaturating purification (Immobilized metal affinity chromatography) on ÄKTA™ Pure M2 system (GE Healthcare) fitted with HisTrap™ HP 5 mL column (Cytiva). Buffers used for denaturating purification were:

- Buffer A: 6 M urea, 0.5 M NaCl, 10 mM imidazole, 50 mM Tris-HCl, pH 8.0
- Elution buffer B: 6 M urea, 0.5 M NaCl, 0.5 M imidazole, 50 mM Tris-HCl, pH 8.0

The column was equilibrated using 4 CV of buffer A, washed with 4 CV of buffer B and reequilibrated with 4 CV of buffer A. The sample was loaded using a sample pump at flow rate of 1 ml/min. The flow-through fraction was gathered and stored on ice as soon as the UV signal started to rise. After that, buffer A was used for the equilibration of the column until the UV signal returned to its baseline value. Impurities and unwanted proteins were removed using 10 % buffer B, and the corresponding fraction was collected. Recombinant ferritin II was eluted using an increasing gradient of buffer B for 20 minutes. Monitoring the UV signal, the peak was collected in 1 ml fractions. Fractions were analysed using SDS-PAGE electrophoresis. All samples for SDS-PAGE analysis were prepared by mixing 30 µl of sample and 10 µl of 4x SDS-PAGE sample buffer and boiling at 95 °C for 5 minutes.

2.14 Refolding

Peak fractions from denaturating purification were pooled together and refolded. During step-down refolding, the concentration of urea was decreasing. The concentration of the sample was set to 0.2 mg/ml by dilution in buffer A and β-mercapthoethanol was added in ratio 2 µl to 10 ml of sample. All dialysis step was done at 4 °C. Solutions for step-down refolding were:

- solution I: 6 M urea, 150 mM NaCl, 50 mM Tris-HCl, 2 mM β-mercapthoethanol, pH 9.0
- solution II: 20% glycerol, 150 mM NaCl, 50 mM Tris-HCl, 2 mM β-mercapthoethanol, pH 9.0
- solution III: 150 mM Tris-HCl, 150 mM NaCl, pH 9.0

Sample was placed into SnakeSkin™ Dialysis Tubing 10.000 MWCO (Thermo Scientific), and the tube was placed into the beaker with 100 ml of solution I and 100 ml of solution II. Dialysis solution was stirred overnight. The next day, 100 ml of dialysis solution was replaced with 100 ml of solution II. After stirring for 8 hours, the step was repeated. The following day 100 ml of dialysis solution was replaced with 100 ml of solution III and dialysed for 8 hours. Following again with replacement of 100 ml dialysis solution with 300 ml of solution III. The next day, the dialysis solution was exposed to the 1 l of solution III and dialyzed for 8 hours. At the end of the refolding, sample was removed from the dialysis tube and spined down at 13 000 for 10 minutes. Concentration of supernatant was measured with NanoPhotometer® Pearl (Implen). Supernatant was filtered through 0.22 µm filter and prepared for SDS-PAGE analysis by mixing 30 µl of sample and 10 µl of 4x SDS-PAGE sample buffer and boiling at 95 °C for 5 minutes.

2.15 Size-exclusion chromatography

Samples from refolding were analysed using size-exclusion chromatography to further purify recombinant ferritin II on the column and find out protein molecular weight and protein aggregation with DLS (Dynamic Light Scattering). Superdex 200 Increase 10/300 GL column was tested for optimalization of protein purification, which has a range between 10 000 to 600 000 molecular weights.

2.15.1 Superdex 200 Increase 10/300 GL

The sample was concentrated using Amicon® Ultra-4 Centrifugal Filter unit with 3K cut-off (Merck Millipore) from 5 ml to 500 µl, spined at 15 000 rpm for 20 minutes prior loading onto Superdex 200 Increase 10/300 GL. The column was washed with water and equilibrated with 1 CV of buffer containing 150 mM Tris-HC and 150 mM NaCl pH 9.0. The sample was applied onto the column and the purification was performed at 0.5 ml/min flowrate. When the UV started to increase, the protein was collected into 0.5 ml fractions. During SEC, DAWN® 8^+ (Wyatt Technology) and Optilab® T-rEX were used for inline verification of protein molecular weight homogeneity. Results were then visualized in software ASTRA (Wyatt Technology). All fractions were analysed with SDS-PAGE electrophoresis.

2.16 Electron microscopy

The sample from size-exclusion chromatography was used for primary screening with electron microscopy (EM). Measurement with EM was done by Ing. Zdenko Gardian, Ph.D. at Laboratory of Electron Microscopy, Faculty of Science, University of South Bohemia. Firstly, negative stain was examined and after particle picking, sample was measured with CryoEM.

2.17 Stability characterization

For obtaining more detailed information about ferritin II stability and aggregation in a wide range of temperatures, ferritin II was measured at Prometheus Panta (NanoTemper). Measurement was done with the assistance of the experts from NanoTemper company. Prometheus Panta gives information about protein thermal unfolding, particle size and aggregation by measuring with four technologies – nanoDSF (nano differential scanning fluorimetry), backreflection, DLS, and SLS (static light scattering).

3 Results

3.1 Cloning into the vectors

By using gradient PCR, the ideal annealing temperature for each primer pair was detected in Figure 8, agarose gel from gradient PCR of vectors pASK-IBA37+ and pETSUMO is visualised from G:BOX Chemi-XX6 (SynGene). Based on the results, the annealing temperature of individual primer pairs was set to 55 °C.

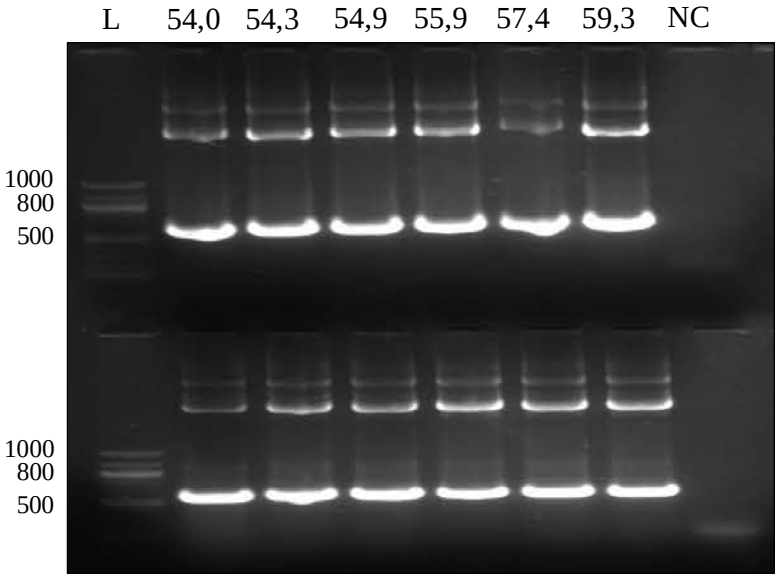

Figure 8: **Gradient PCR of pASK-IBA37+ and pETSUMO vectors**: In the upper part, there is gradient PCR of vector pASK-IBA37+ with inserted ferritin II, in the bottom part, there is pETSUMO vector. All samples were loaded with a volume of 10 µl. L – 100 bp DNA ladder, 54,0 - 59,3 – tested temperatures, NC – negative control without DNA template at 55,9 °C.

The ferritin II amplicons were amplified at selected temperature using Q5® High Fidelity DNA polymerase. After Q5 PCR, each amplicon was cut out from the gel, purified and its concentration was measured (Table 13).

Table 13: Concentration of amplicons and vectors with used amount for cloning

Amplicon	Amplicon concentration [ng/µl]/volume in reaction [µl]	Vector concentration [ng/µl]/volume in reaction [µl]
pASK-IBA37+	83.8/12	243/4
pETSUMO	14.15/2	26.5/4
pET21d	56.11/17,8	314/3,2
pASK-IBA33+	125,1/8	718/1,4

Each amplicon was cloned according to its specific protocol, for pASK-IBA33+, pASK-IBA37+ and pET21d the digestion with a specific restriction enzyme was used and for pETSUMO, NeBuilder cloning was used. NEB® 5-alpha competent *E. coli* cells were transformed by ligation reaction. The following day, 12 colonies and one negative control were picked from plates and analysed by colony PCR using primers from Table 1 for verification of the presence of the required gene. In Figure 9, there are examples of picked colonies of pASK-IBA37+ and pETSUMO vectors, which were then isolated from the minipreps and sequenced. Data of the remaining vectors are in Supplements.

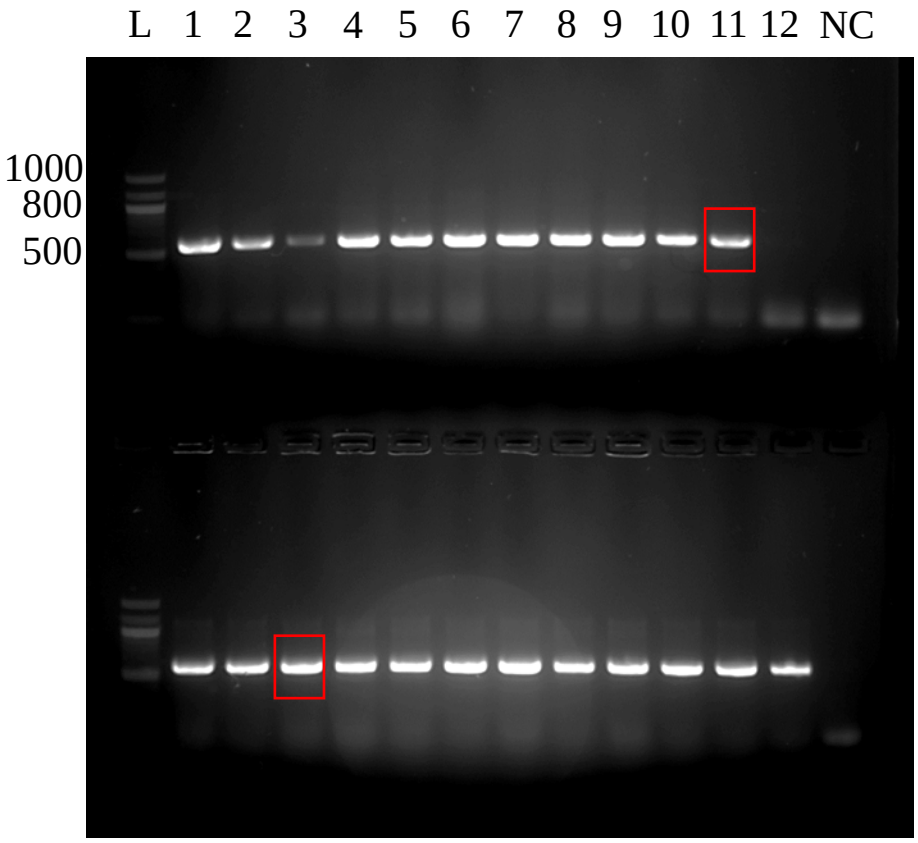

Figure 9: **Colony PCR of ferritin II gene in pASK-IBA37+ and pETSUMO vectors**: In the upper gel, colony PCR with vector is reported pASK-IBA37+, colony 11 was used for further studies. pETSUMO vector is in the bottom part, where colony 3 was picked. L – 100 bp DNA ladder, 1-12 – selective colonies, NC – negative control with no DNA template, red box – picked colonies

After verification of selected colonies for the presence of the gene of interest, maxipreps were prepared. Plasmids from maxipreps were isolated and transformed into several expression strains of *E. coli*.

3.2 Pilot expression

Protein production was optimized during pilot expression for each vector. Different strains of competent *E. coli* cells were tested at different temperatures and concentrations of inducer to optimize protein production. The approximate molecular weight of ferritin II is 24 kDa in all vectors, except for pETSUMO vector, whose estimated molecular weight is 15 kDa, together with insert is approximately 40 kDa.

pASK-IBA37+ and pETSUMO vectors included N-terminal His-tag. Both of them were tested in BL21-CodonPlus(DE3)-RIPL, Rosetta^{TM}(DE3) and ArticExpress(DE3) cells. Expression of ferritin II showed low production in all conditions in the soluble fractions (Figure 10). In the case of pETSUMO vector, the expression of the protein was higher.

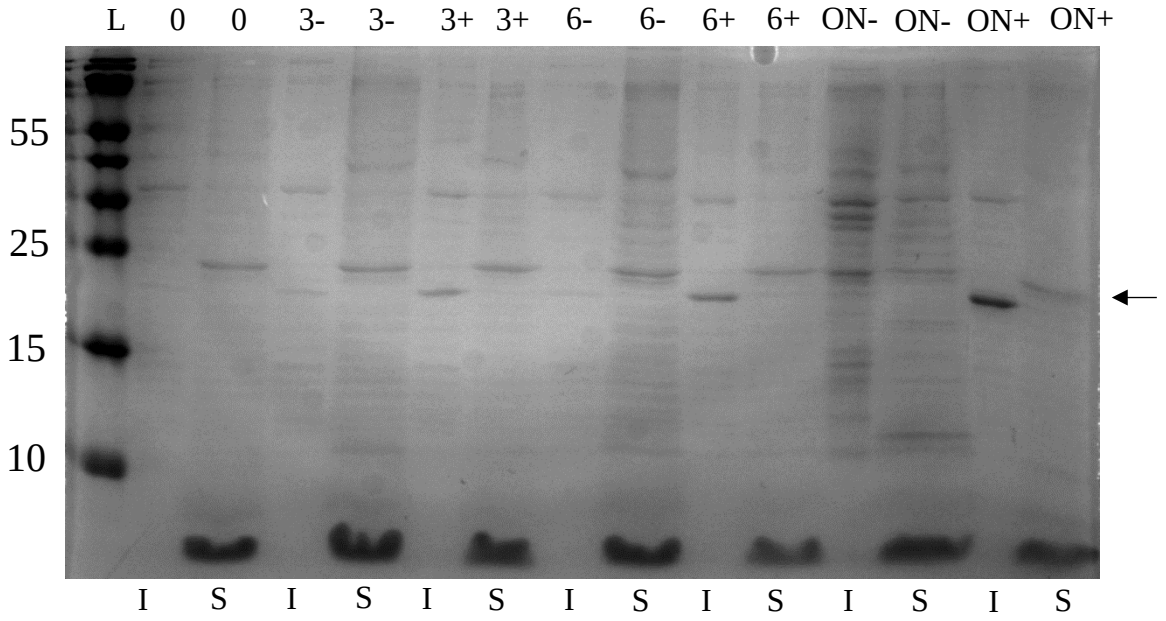

Figure 10: **Pilot expression of ferritin II in pASK-IBA37+** in BL21-CodonPlus cells at 18 °C induced by ATC. L - PageRulerTM Protein Prestained Ladder, number – an hour of harvesting, ON – overnight, - uninduced culture, + induced culture, I – insoluble fraction, S – soluble fraction

The following western blot analysis showed a low concentration of soluble fraction and main production was present in the insoluble fraction. Regardless of different cells, temperatures, times and concentrations, each condition yielded similar production of the insoluble fraction (data in Supplements). pETSUMO vector was chosen for the large-scale expression in ArticExpress(DE3) cells at 13 °C for 24 hours in the presence of 1 mM IPTG (Figure 11) due to the higher presence of protein in soluble fraction according to the western blot analysis results (Figure 12).

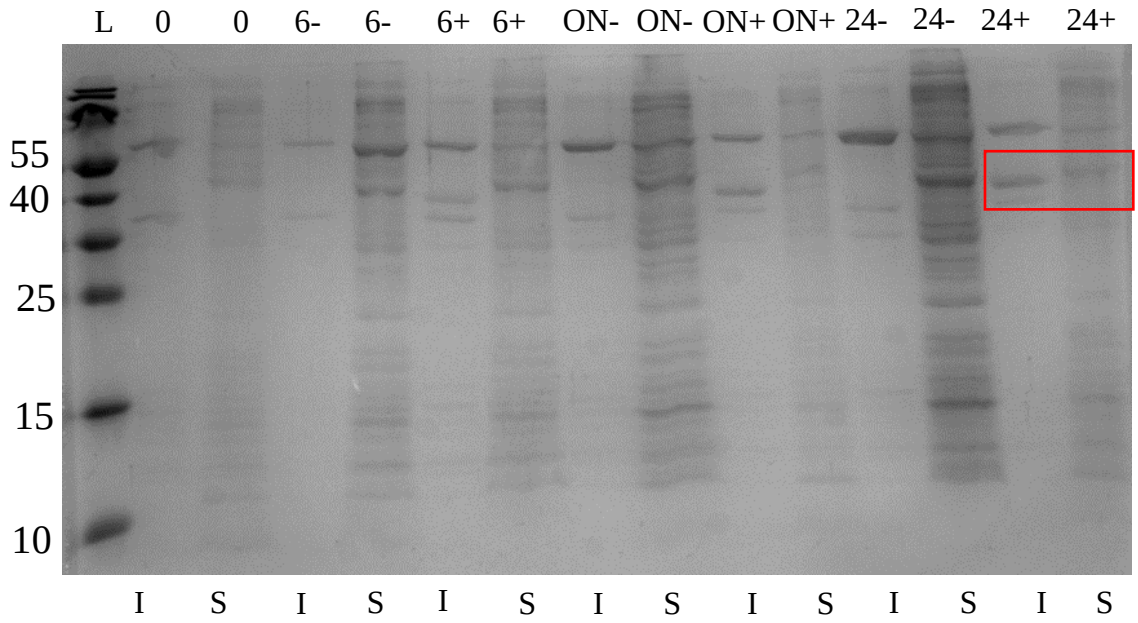

Figure 11: **Pilot expression of ferritin II in pETSUMO** in ArticExpress(DE3) cells at 13 °C induced by 0.5 mM IPTG. L - PageRulerTM Protein Prestained Ladder, number – an hour of harvesting, ON – overnight, - uninduced culture, + induced culture, I – insoluble fraction, S – soluble fraction, red box – chosen conditions for large-scale expression

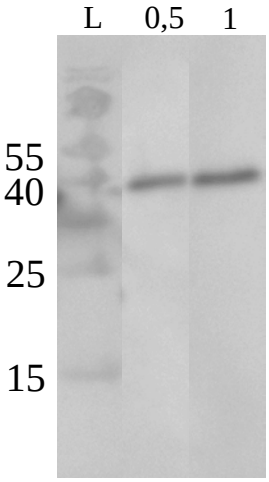

Figure 12: **Westernblot of ferritin II in pETSUMO** in ArticExpress(DE3) cells at 13 °C induced by IPTG. L - PageRulerTM Protein Prestained Ladder, 0.5/1 – concentration of IPTG in mM

Vector without N-terminal His-tag pET21d was tested using two different competent cells - BL21-CodonPlus(DE3)-RIPL and ArticExpress(DE3). Expression in BL21-CodonPlus cells (Figure 13, 14) showed similar results as in pETSUMO and pASK-IBA37+ vectors (data in Supplements). No production was detected in the soluble fraction, however, production in the insoluble fraction was high. Based on the results, significant features of BL21-CodonPlus(DE3) cells showed no relevant effects on the

production, and BL21(DE3) cells were used for large expression. Expression in ArticExpress(DE3) cells showed no significant production.

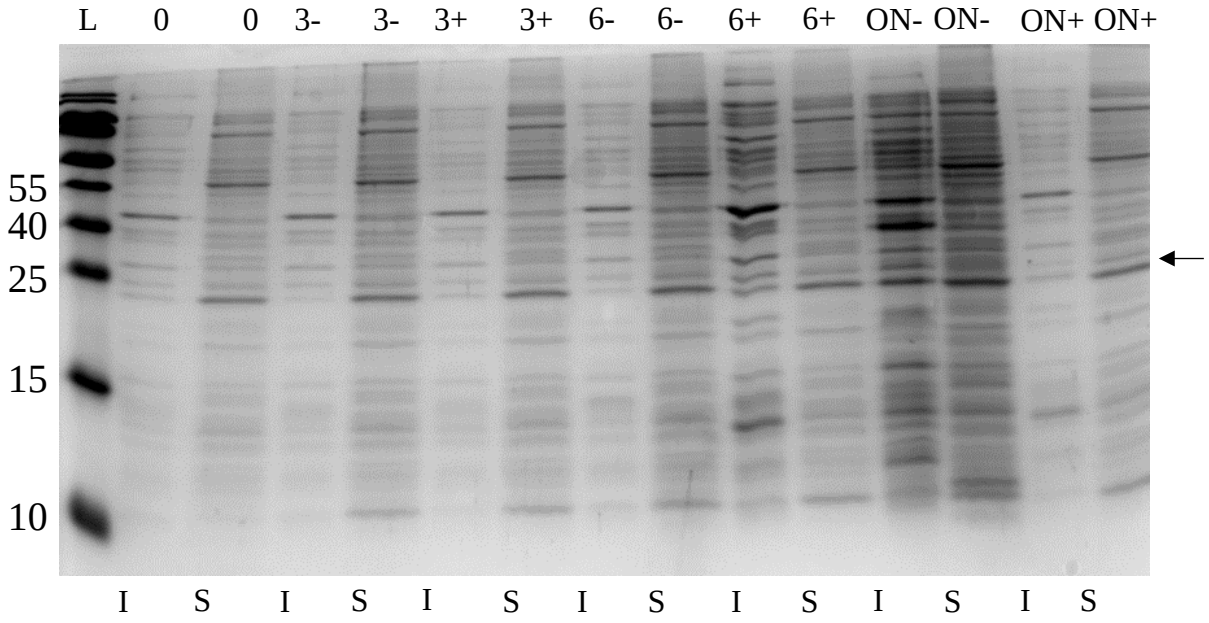

Figure 13: **Pilot expression of ferritin II in pET21d** in BL21-CodonPlus cells at 16 °C induced by 1 mM IPTG. L - PageRulerTM Protein Prestained Ladder, number – an hour of harvesting, ON – overnight, -uninduced culture, + induced culture, I – insoluble fraction, S – soluble fraction

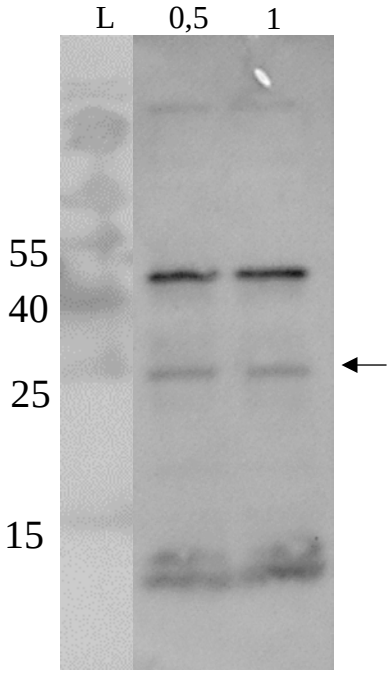

Figure 14: **Westernblot analysis of ferritin II in pET21d** in BL21-CodonPlus cells at 16 °C induced by IPTG. L - PageRulerTM Protein Prestained Ladder, 0.5/1 – concentration of IPTG in mM

Table 14: Summary of all results from pilot expression

Competent cells	Plasmid	Inducer	Antibiotics resistance	Temperature [° C]	Time interval in hours	Protein production insoluble	Protein production soluble
BL21-CodonPlus(DE3)-RIPL	pASK-IBA37+	ATC	AMP	18	3, 6, ON	+	-
				37	2, 4, 6	+	-
	pETSUMO	IPTG	CAN	18	3, 6, ON	-	+
				37	2, 4, 6	-	+
	pET21d	IPTG	AMP	16	3, 6, ON	-	-
				37	2, 4, 6	-	-
Rosetta™(DE3)	pASK-IBA37+	ATC	AMP	18	3,6, ON	+	-
				37	2, 4, 6	+	-
	pETSUMO	IPTG	CAN	18	3,6, ON	-	-
				37	2, 4, 6	-	-
ArticExpress(DE3)	pASK-IBA37+	ATC	AMP	13	6, ON, 24	-	-
	pETSUMO	IPTG	CAN	13	6, ON, 24	+	-
	pET21d	IPTG	AMP	13	6, ON, 24	+	-

3.3 Large-scale expression

Vector pETSUMO, which was chosen for large-scale expression of soluble fraction, did not produce any soluble protein (Figure 15). It showed that large volumes have effects on protein folding and apparently protein is not capable to remain soluble.

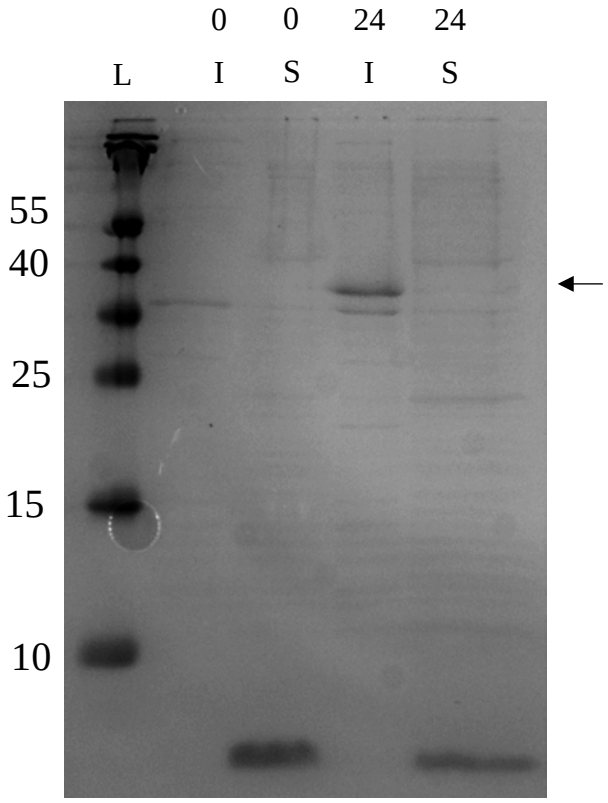

Figure 15: **Large-scale expression of ferritin II in pETSUMO** in ArticExpress(DE3) cells at 13 °C induced by 1 mM IPTG, L - PageRulerTM Protein Prestained Ladder, I – insoluble fraction, S – soluble fraction, 0/24 – and hour of harvesting

Due to almost no production of protein in the soluble fraction, steps for the improvement of the expression of pET100, pET21d and pASK-IBA33+ vectors were applied. Expression of protein with additional glucose step in BL21(DE3) cells showed no production in pET21d and pASK-IBA33+ vectors. Glucose probably did not influence the expression of protein without N-terminal His-tag. The same results were seen during expression with supplementation with iron (Figure 16). The only production was observed in vector pET100 mainly in the insoluble fractions. Based on these facts, vector pET100 was chosen for the following studies.

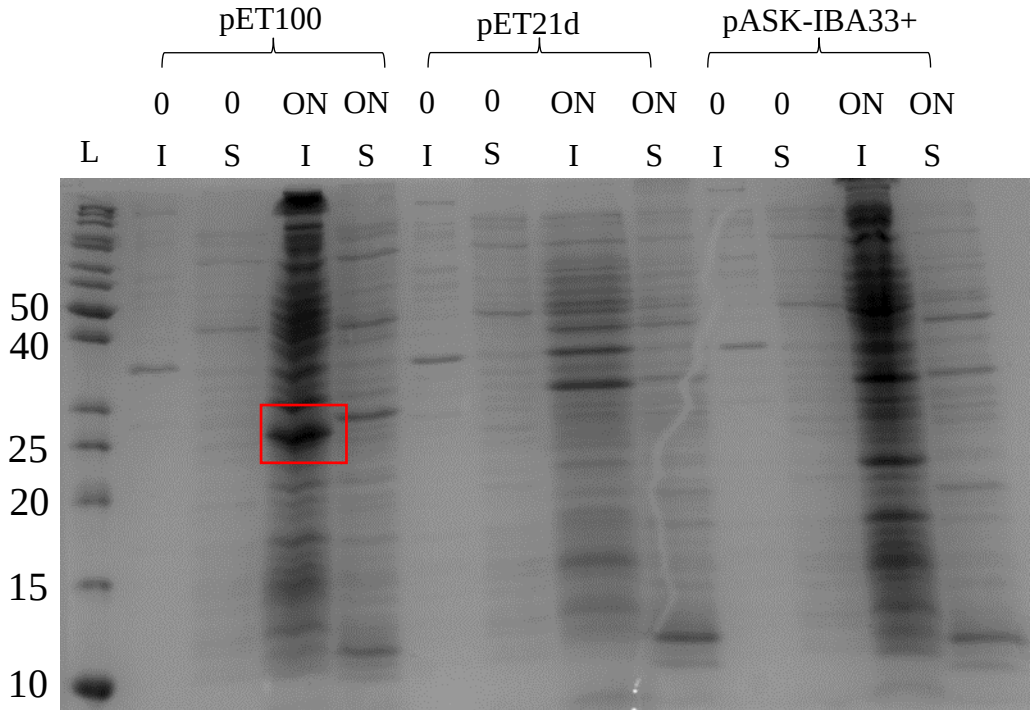

Figure 16**: Expression of ferritin II with iron supplementation in pET100, pET21d, pASK-IBA33+** in BL21(DE3) cells at 30 °C induced by 1 mM IPTG or ATC. L - PageRulerTM Protein Unstained Ladder, 0 – uninduced culture, ON – overnight harvesting, I – insoluble fraction, S – soluble fraction

3.4 Denaturating purification

After large-scale expression of ferritin in pET100 vector, cells were harvested and lysed in LM20 Microfluidizer® Processor (Microfluidics). Centrifugated pellet was stirred overnight in a buffer containing guanidine hydrochlorid. For separation and clarification of inclusion bodies, centrifugation was used. Ferritin II in vector pET100 was purified using its N-terminal HisTag with HisTrap column-Ni^{2+}. Supernatant from isolation of inclusion bodies was loaded onto the column and purified using gradient elution. Protein started to elute in the presence of 43.5 % buffer B (Figure 17). Fractions with volume of 1 ml were collected and analysed with SDS-PAGE electrophoresis (Figure 18). Fractions 2-7 were pooled, and concentration of the final sample was 0.784 mg/ml, $A_{260/280} = 0.77$.

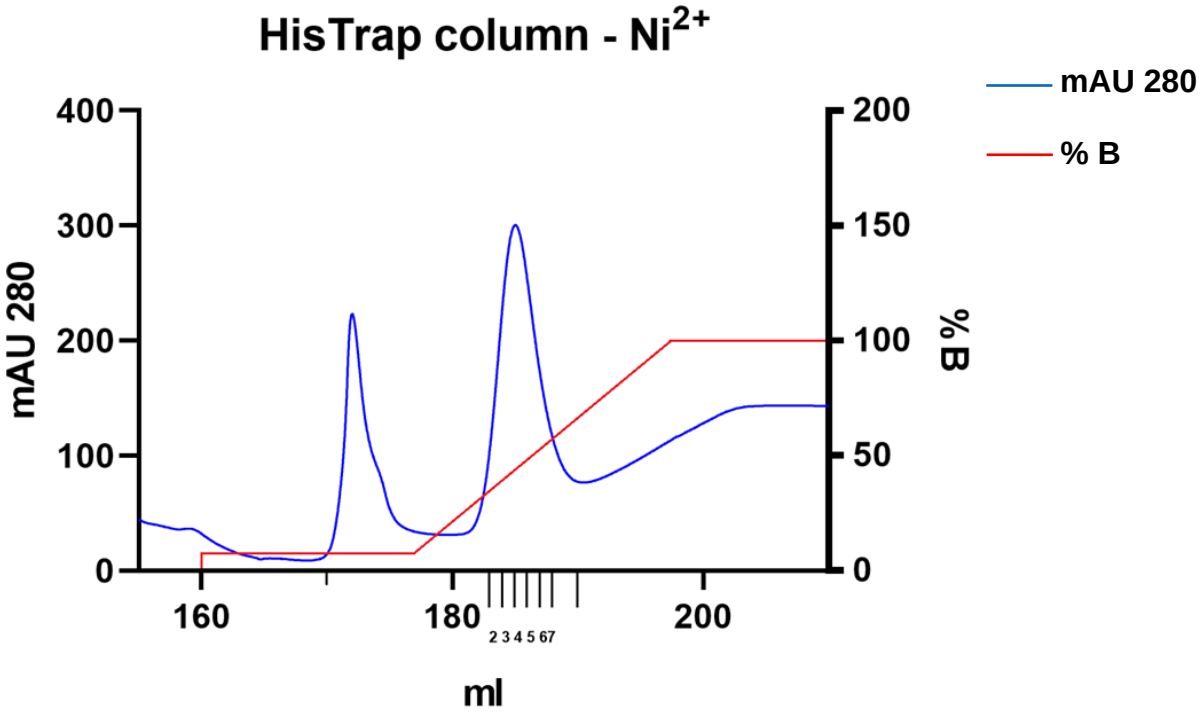

Figure 18: **Denaturating purification chromatogram of ferritin II with pET100** (blue line) on HisTrap column-Ni^{2+} with gradient elution with buffer B (red line). 2-7 – collected fraction.

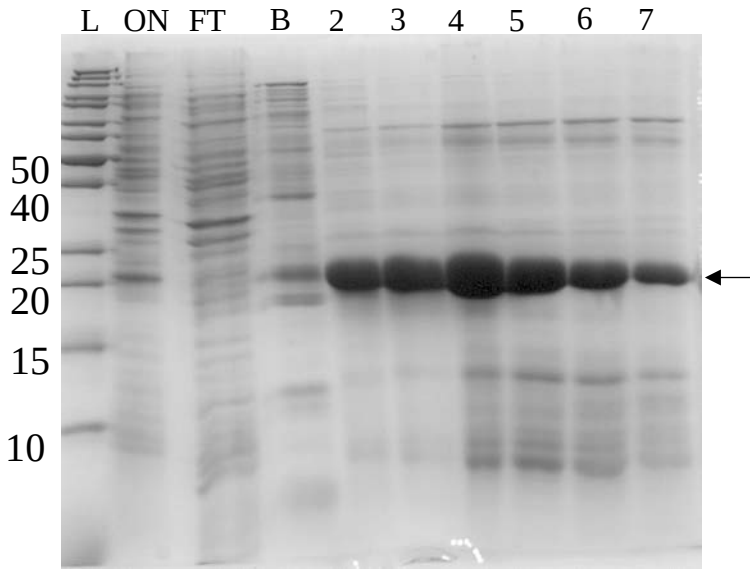

Figure 17: **Denaturating purification of ferritin II in pET100.** L - PageRulerTM Protein Unstained Ladder, ON – sample loaded onto column, FT – flow through fraction, B - eluate with 10% buffer B, number – eluted fraction

3.5 Refolding

Sample of each fraction from denaturating purification was diluted in buffer B to approximately 0.2 mg/ml. Sample was loaded into the dialysis tube and placed into the

solution containing 6 M urea. Concentration of urea gradually decreased during refolding. Samples before and after refolding were analysed with SDS-PAGE electrophoresis (Figure 19). SDS-PAGE proven presence of protein with the corresponding size 24 kDa. The protein concentration of the sample from refolding was 0.147 mg/ml, $A_{260/280}$=0.47.

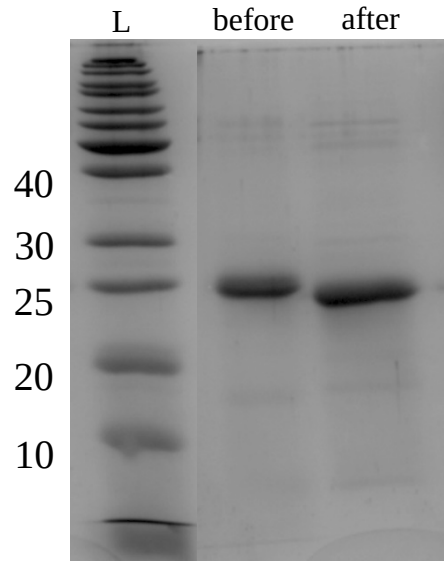

Figure 19: **Refolding of pET100:** L - PageRulerTM Protein Unstained Ladder, before – diluted sample before refolding, after – sample after refolding

3.6 Superdex 200 Increase 10/300 GL

Before purification, the protein was concentrated using Amicon® Ultra-4 Centrifugal Filter unit with 3K cut-off and centrifugated to get rid of precipitation at 15 000 rpm for 20 minutes. 500 µl of sample was loaded on the Superdex 200 Increase 10/300 GL (Figure 20). Fractions with a volume of 500 µl were collected and analysed with SDS-PAGE electrophoresis (Figure 21).

Results visualised in software ASTRA with DLS showed that in peak 1 is probably presence of aggregation due to the low homogeneity of the sample (data in Supplements). Molecular weight of the peak 1 was higher and did not correspond with the presumed one. On the other hand, consumption of peak 2 is much more consistent and its molecular weight is approximately 600 kDa. Fractions B2-B4 were pooled (0.089 mg/ml, $A_{260/280}$ = 0.88) and used for future studies.

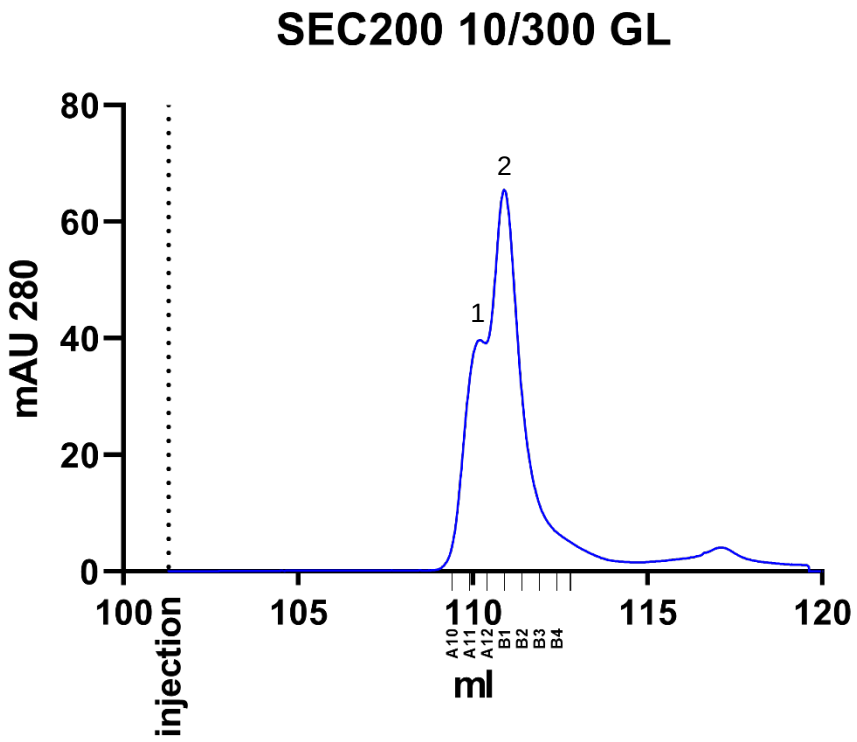

Figure 21: **Size-exclusion purification chromatogram of ferritin II in pET100** on SEC200 10/300 GL column, A10-B4 – collected fractions.

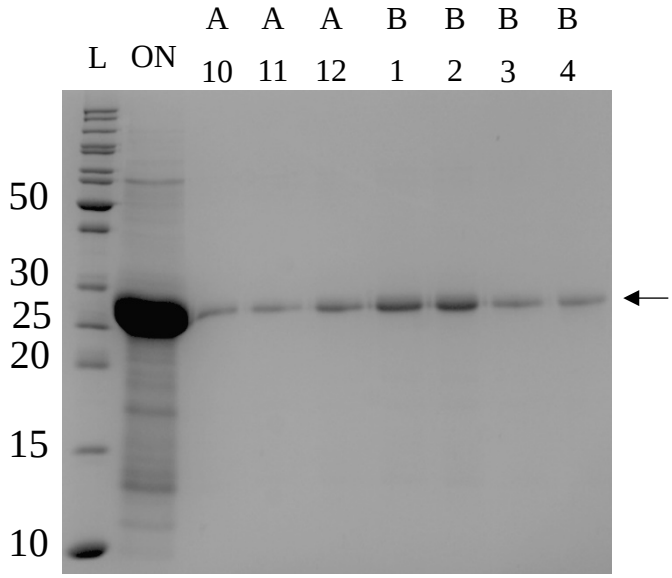

Figure 20: **Size-exclusion purification of ferritin II in pET100** on SEC200 10/300, L - PageRulerTM Protein Unstained Ladder, ON – sample loaded onto column, FT – flow through fraction, A10-B4 – eluted fractions

3.7 Electron microscopy

The sample from size-exclusion chromatography was concentrated using Amicon® Ultra-4 Centrifugal Filter unit with 3K cut-off to approximately 0.2 mg/ml. Firstly, the sample was examined with negative stain, where particles were picked up (Figure 22). All particles had a similar characteristic square shape.

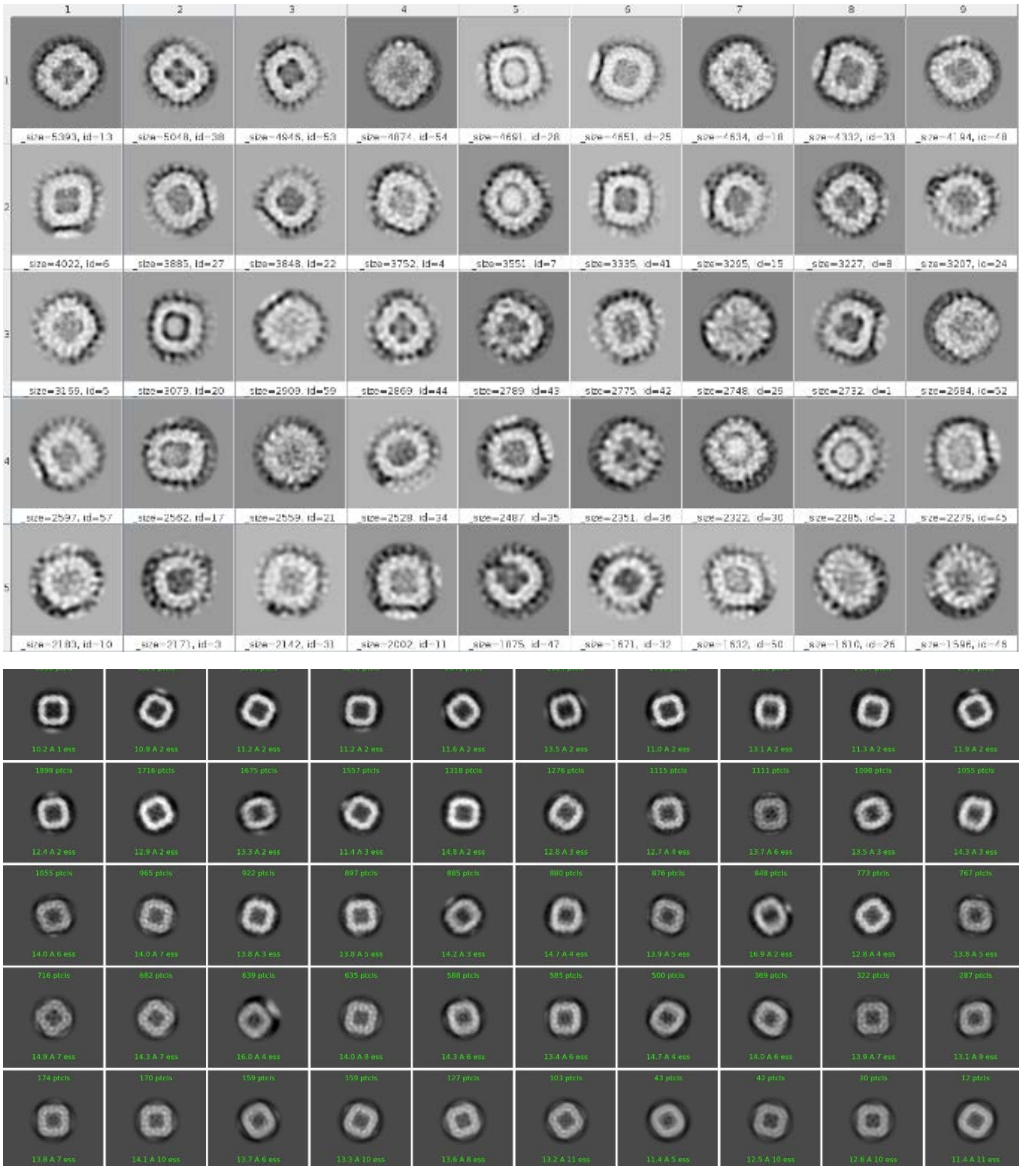

Figure 22: **Particle picking from negative stain of ferritin II (upper part) and from CryoEM (bottom part)**

This sample was used for obtaining preliminary data from CryoEM, which proved that ferritin II possesses a conserved structure like other ferritins. The resulting particle

image from CryoEM is perfectly symmetric (Figure 23). The initial resolution of about 9 Å was reached. The CryoEM measurements are still ongoing in order to obtain better resolution data.

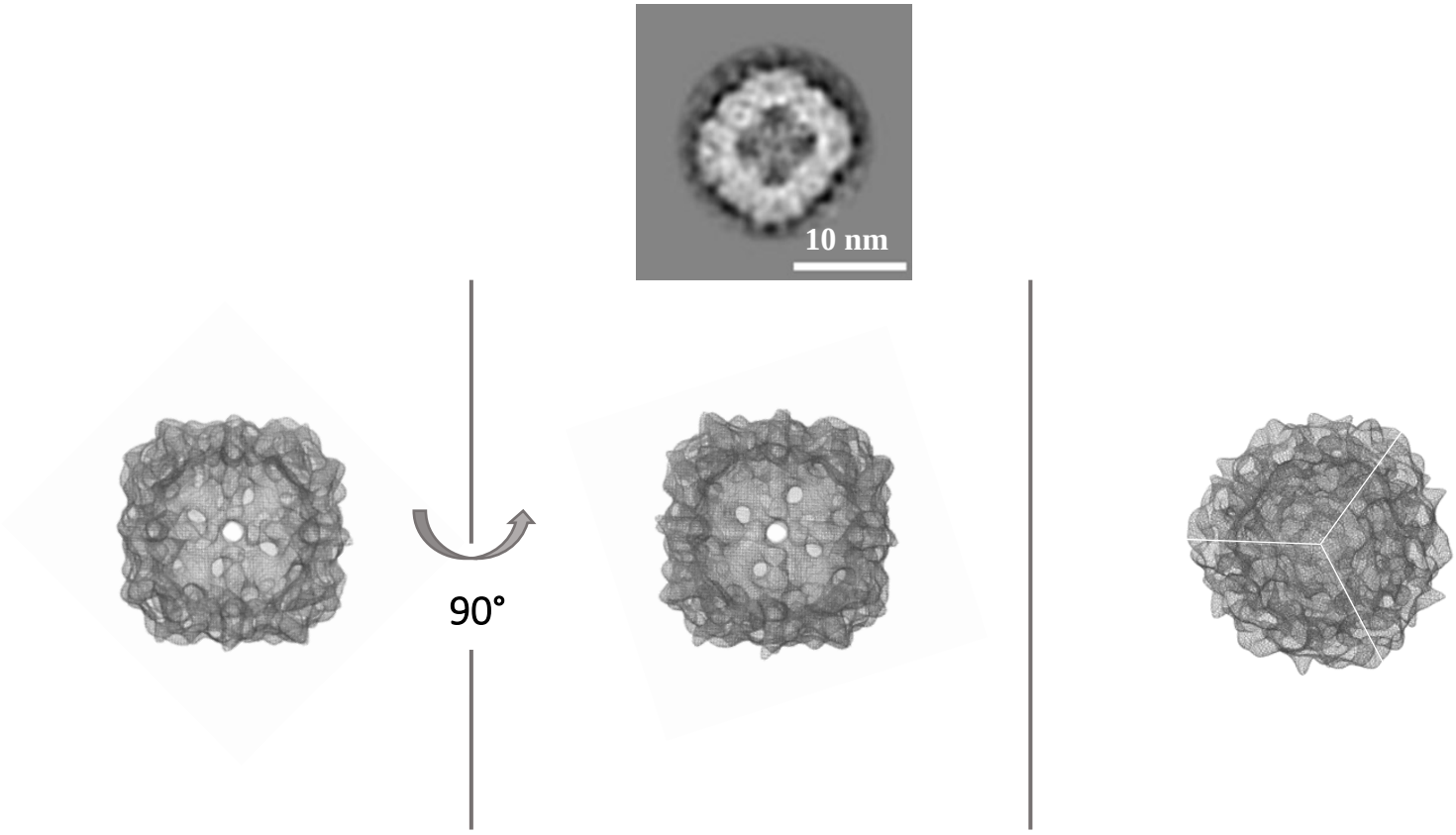

Figure 23: **Images from CryoEM from initial measurement of ferritin II** from different angle and in the upper part is the real image of ferritin II from CryoEM with scalebar.

3.8 Stability characterization

The sample obtained from size-exclusion chromatography was concentrated using Amicon® Ultra-4 Centrifugal Filter unit with 3K cut-off to approximately 0.3 mg/ml and measured by Prometheus Panta (NanoTemper). Measurement showed that ferritin II is relatively stable from 30 °C to 90 °C. Above 90 °C, the ratio 350/330 nm started to increase and the cumulant radius is less stable, which shows that some particles of protein started to lose their stability and melt. This proved that the theoretical melting temperature of ferritin is about 106 °C.

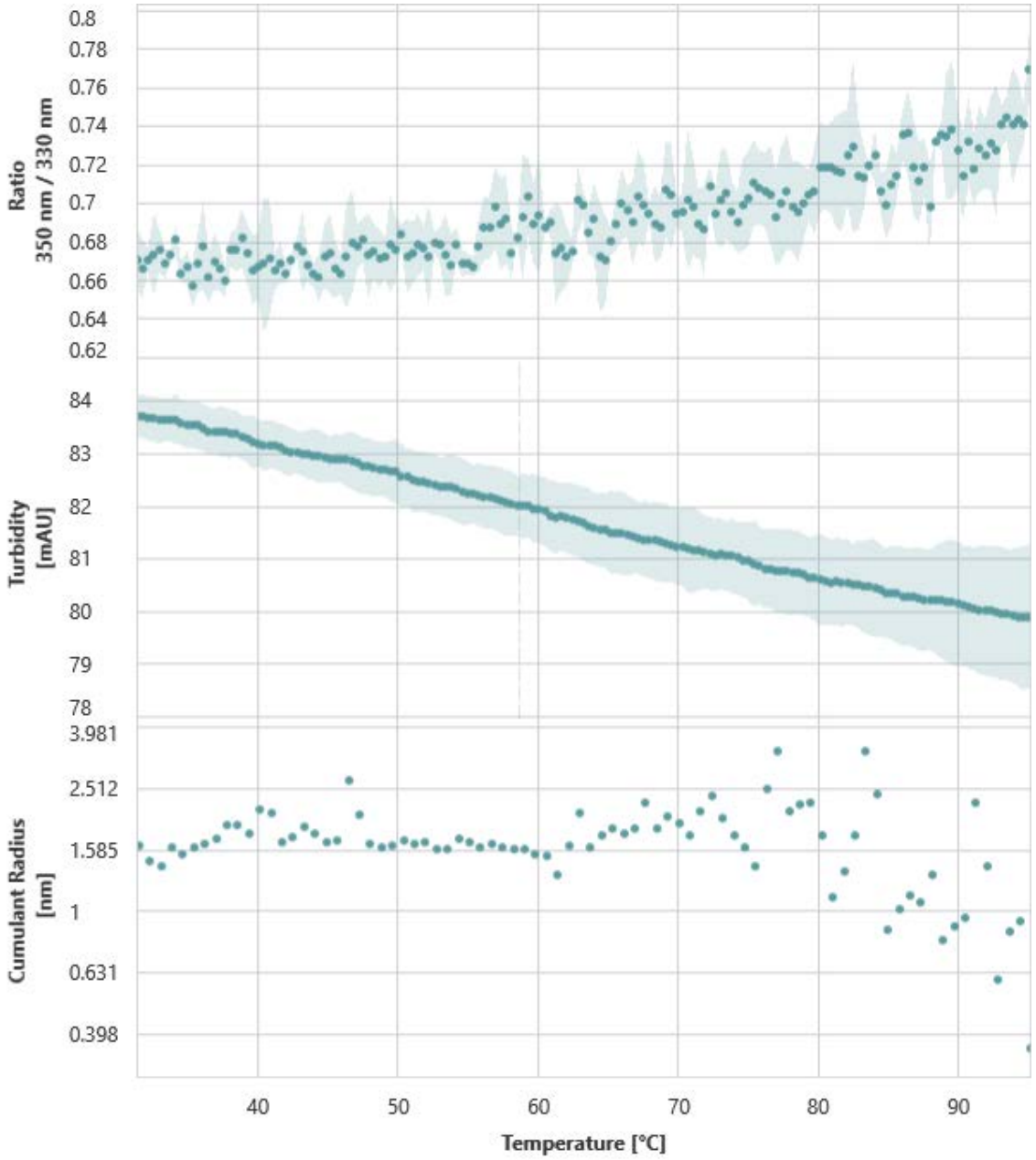

Figure 24: **Measurement of melting point of ferritin II with Prometheus Panta**

Probability of aggregation was measured using Prometheus Panta with increasing temperature. In the sample, particles with about 9 nm were mostly present, which corresponds to the required ferritin II size without any significant/measurable aggregation. The relative probability of aggregation was low, however, the minority of aggregates with about 700 nm radius were also present.

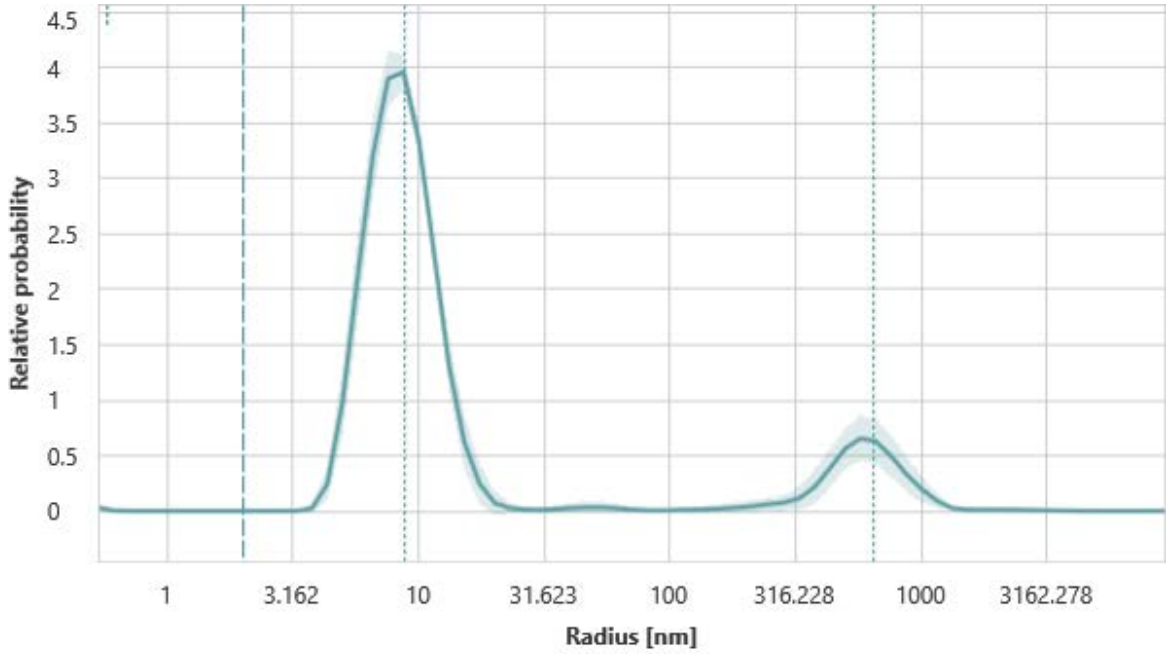

Figure 25: **Size analysis of ferritin II with Prometheus Panta**

4 Discussion

Despite the significance of ticks as disease vectors, it is still very little known about ticks´ biochemistry compared to other insects. Iron metabolism research is still at an early stage. Ticks transmit different types of pathogens and due to the increasing number of incidents, it is necessary to prevent transmission by stopping ticks to feed host blood. Vaccine targeted to the ticks could avert ticks feeding host blood and realising pathogens. Ferritin II could be an appropriate candidate for developing the vaccine. Structure determination followed by its functional determination is based on obtaining purified protein in the needed concentration. In this work, the production and purification of ferritin is reported.

For *in vitro* study, several different kinds of *E. coli* strains with various conditions were tested for expression of each vector. It appeared that advantages of several competent cells do not have an effect on the production and BL21(DE3) cells proved to be the most beneficial for the production of ferritin. Several studies dealing with the production of ferritin from *Ornithodoros moubata* [48], a marine invertebrate *Chaetopterus* [51], or from soybeans [40] etc., used the same strain. BL21(DE3) cells are often used for high-level protein expression, easy induction, and production of toxic proteins. Ferritins could be toxic for some competent cells because of their iron core, due to it, BL21(DE3) cells are widely used for production of ferritins. However, the production of ferritin II in the soluble fraction was unsuccessful and the only option was inclusion bodies. Nevertheless, ferritins from different organisms are produced exclusively in inclusion bodies followed by sonication and refolding. So, it is probably highly demanding for ferritin to be produced in soluble fraction. The same method was used for producing ferritin II from *Haemaphysalis flava* (Acari: *Ixodidae*). In the study, they cloned ferritin II into the pET-32a(+) vector and transformed it into the BL21(DE3) competent cells [52].

In this thesis, one of the original aims was to produce ferritin II without His-tag, for this reason, two vectors pASK-IBA33+ and pET21d were tested. However, even the supplementation with iron, which should stabilize the structure, did not help ferritin to fold properly and therefore enable the production of the protein. Ferritin is probably dependent on the His-tag to fold properly in *in vitro* model, pTNT vector was used in the expression study of human H ferritin. The vector is very similar to the pET100 vector, both of them are

used for bacterial expression with His-Tag and contained T7 promoter for sequencing [36]. Only ferritin SFER4 from soybeans was successfully cloned and produced in the untagged vector pET21d, which was also used in this thesis. The following methods for cloning and expression were similar to the ones used in this thesis, however, differences in the organism could cause, that ferritin II from a tick is challenging to produce without His-tag [40]. Ferritin from kuruma prawn (*Marsupenaeus japonicus*) was cloned into the pET21b and the production was conducted in BL21(DE3) cells with the induction of IPTG [53]. For this protein, the pET21b vector was used, which has similar properties as pET21d just with His-tag. This vector with inserted ferritin was expressed in BL21(DE3) at 20 °C with IPTG. Isolation of inclusion bodies was done with sonication and extraction with phosphate-buffered saline supplemented with protease inhibitor. Purification was done with ammonium sulfate precipitation anion exchange chromatography and size-exclusion chromatography with Superdex 200 pg 16/60 column. Buffer for purification contained 10 mM Tris-HCl and 150 mM NaCl [53].

Compared to the production of ferritin I from *Ixodes ricinus*, the methods were the same. Both ferritins were cloned into the vector with His-tag. Instead of DH5alpha cells, ferritin I was cloned into the TOPO 10 F´ cells and the sequence was verified with T7 sequencing primer. For overexpression, BL21(DE3) cells were used with ampicillin and chloramphenicol resistance. After inducing with 1 mM IPTG, cells were harvested after 4 hours, instead of 16 hours. Harvested cells were resuspended in a similar buffer containing 6 M guanidine hydrochloride. Lysis of the cells was done using liquid nitrogen and ultra-sonication. Denaturating purification was done with buffer including high molar of urea (8 M), however, elution was not done with a high concentration of imidazole. In the study, they used low pH buffer with additional washing steps using buffers with different pH, elution was done with a buffer of pH 4.0. To get rid of the urea, dialysis against 10 mM Tris-HCl, pH 8.0 and 0,1 % (v/v) Triton X-100 was done. Size-exclusion chromatography was done on the column Superose 6 HR 10/300 [48].

Preliminary data from CryoEM showed that ferritin II from *Ixodes ricinus* has similar structure to other ferritins. Compared to another image of ferritins and apo-ferritins from different studies (Figure 26), it is visible that the typical squared shape is conserved, and all ferritins share the same fold, which is highly symmetrical and very similar in size. For example, human apo-ferritin was solved to the resolution of 2.5 Å by CryoEM [54]. For

optimal structure, it is necessary to lower the resolution from 9 Å to be able to model the structure of ferritin II.

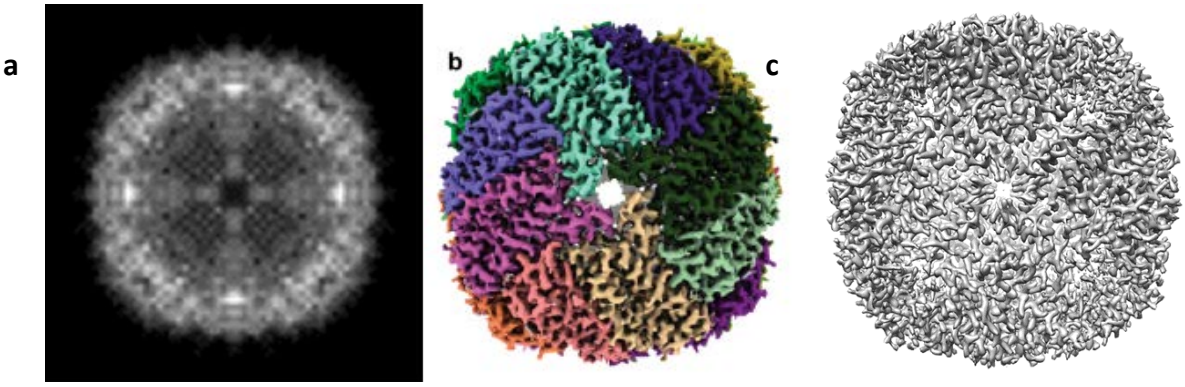

Figure 26: **Examples of images and structures of ferritins from CryoEM: (a)** Image of human heavy chain ferritin [59], **(b)** Structure of human ferritin isoform determined by CryoEM at 2.86 Å resolution [60], **(c)** CryoEM image of horse spleen apoferritin [61].

5 Conclusion

In conclusion, ferritin II from Ixodes ricinus was cloned into five different vectors, amplified, and digested with several enzymes or with NEBuilder® HiFi DNA Assembly. For large expression, different conditions were tested, and the expression was not successful in soluble fraction. Pilot expression and additional enhancement during expression showed low production of ferritin II in vectors without His-tag. In order to obtain certain amount of the pure protein for the following studies, the pET100 vector was chosen for large-scale expression into inclusion bodies. Inclusion bodies were isolated and purified with denaturating purification and refolded. The ferritin II from *Ixodes ricinus* was obtained from size exclusion chromatography and the sample was tested using CryoEM technique. Obtained results confirmed the correct form of protein.

6 References

[1] FRANCISCHETTI, Ivo,, Anderson SA-NUNES, Ben MANS, Isabel SANTOS a Jose RIBEIRO. The role of saliva in tick feeding. *Frontiers in Bioscience* [online]. 2009, (14), 2051-2088 [cit. 2022-12-30]. ISSN 10939946. doi:10.2741/3363

[2] JONGEJAN, F. a G. UILENBERG. The global importance of ticks. *Parasitology* [online]. 2004, **129**(1), 3-14 [cit. 2022-12-30]. ISSN 0031-1820. doi:10.1017/S0031182004005967

[3] MEDLOCK, Jolyon, Kayleigh HANSFORD, Antra BORMANE et al. Driving forces for changes in geographical distribution of Ixodes ricinus ticks in Europe. *Parasites & Vectors* [online]. 2013, **6**(1) [cit. 2022-12-30]. ISSN 1756-3305. doi:10.1186/1756-3305-6-1

[4] BARKER, S. C. a A. MURRELL. Systematics and evolution of ticks with a list of valid genus and species names. *Parasitology* [online]. 2004, **129**(1), 15-36 [cit. 2023-02-14]. ISSN 0031-1820. doi:10.1017/S0031182004005207

[5] HOSKINS, J.D. a E.W. CUPP. Ticks of veterinary importance I.: The Ixodidae family: identification, behavior, and associated diseases. *The Compendium on continuing education for the practicing veterinarian*. USA, 1988, **10**(5), 564. ISSN 0193-1903.

[6] SONENSHINE, Daniel a R. ROE. *Biology of Ticks*. Second Edition. New York: Oxford University Press, 2014. ISBN 978-0199744060.

[7] LOUI MONFARED, Ali, Mohammad MAHMOODI a Roohollah FATTAHI. Prevalence of ixodid ticks on cattle, sheep and goats in Ilam County, Ilam Province, Iran. *Journal of Parasitic Diseases* [online]. 2015, **39**(1), 37-40 [cit. 2023-02-21]. ISSN 0971-7196. doi:10.1007/s12639-013-0267-8

[8] PIESMAN, Joseph a Lars EISEN. Prevention of Tick-Borne Diseases. *Annual Review of Entomology* [online]. 2008, **53**(1), 323-43 [cit. 2023-02-23]. ISSN 0066-4170. doi:10.1146/annurev.ento.53.103106.093429

[9] SAJID, M.S., Z. IQBAL, M.N. KHAN, G. MUHAMAMD a M.U. IQBAL. Effect of Hyalomma Ticks (Acari: Ixodidae) on Milk Production of Dairy Buffaloes (Bos Bubalus Bubalis) of Punjab (Pakistan). *Italian Journal of Animal Science* [online]. 2016, **6**(2), 939-941 [cit. 2023-02-21]. ISSN 1828-051X. doi:10.4081/ijas.2007.s2.939

[10] RANDOLPH, S.E., L. GERN a P.A. NUTTALL. Co-feeding ticks: Epidemiological significance for tick-borne pathogen transmission. *Parasitology Today* [online]. 1996, **12**(12), 472-479 [cit. 2023-02-23]. ISSN 01694758. doi:10.1016/S0169-4758(96)10072-7

[11] RIBEIRO, José M.C. a Jesus G. VALENZUELA. Vector Biology. *Tropical Infectious Diseases: Principles, Pathogens and Practice* [online]. Elsevier, 2011, 45-51 [cit. 2023-02-15]. ISBN 9780702039355. doi:10.1016/B978-0-7020-3935-5.00008-2

[12] STANEK, Gerald a Franc STRLE. Lyme borreliosis. *The Lancet* [online]. 2003, **362**(9396), 1639-1647 [cit. 2023-02-23]. ISSN 01406736. doi:10.1016/S0140-6736(03)14798-8

[13] HUBÁLEK, Zdenek a Ivo RUDOLF. Tick-borne viruses in Europe. *Parasitology Research* [online]. 2012, **111**(1), 9-36 [cit. 2023-02-21]. ISSN 0932-0113. doi:10.1007/s00436-012-2910-1

[14] LANI, Rafidah, Ehsan MOGHADDAM, Amin HAGHANI, Li-Yen CHANG, Sazaly ABUBAKAR a Keivan ZANDI. Tick-borne viruses: A review from the perspective of therapeutic approaches. *Ticks and Tick-borne Diseases* [online]. 2014, **5**(5), 457-465 [cit. 2023-02-23]. ISSN 1877959X. doi:10.1016/j.ttbdis.2014.04.001

[15] MANSFIELD, K. L., N. JOHNSON, L. P. PHIPPS, J. R. STEPHENSON, A. R. FOOKS a T. SOLOMON. Tick-borne encephalitis virus – a review of an emerging

zoonosis. *Journal of General Virology* [online]. 2009, **90**(8), 1781-1794 [cit. 2023-02-23]. ISSN 0022-1317. doi:10.1099/vir.0.011437-0

[16] BRAKS, Marieta, Sipke WIEREN, Willem TAKKEN a Hein SPRONG. *Ecology and prevention of Lyme borreliosis* [online]. 4. Ecology and Control of Vector-borne diseases, 2016 [cit. 2022-12-30]. ISBN 978-90-8686-838-4. https://doi.org/10.3920/978-90-8686-838-4

[17] CUPP, Eddie W. Biology of Ticks. *Veterinary Clinics of North America: Small Animal Practice* [online]. 1991, **21**(1), 1-26 [cit. 2022-12-30]. ISSN 01955616. doi:10.1016/S0195-5616(91)50001-2

[18] OLIVER, J H. Biology and Systematics of Ticks (Acari: Ixodida). *Annual Review of Ecology and Systematics* [online]. 1989, **20**(1), 397-430 [cit. 2022-12-30]. ISSN 0066-4162. doi:10.1146/annurev.es.20.110189.002145

[19] GERN, Lise. Life Cycle of Borrelia burgdorferi sensu lato and Transmission to Humans. *Lyme Borreliosis* [online]. Basel: KARGER, 2009, **37**, 18-30 [cit. 2022-12-30]. Current Problems in Dermatology. ISBN 978-3-8055-9114-0. doi:10.1159/000213068

[20] HENTZE, Matthias, Martina MUCKENTHALER a Nancy ANDREWS. Balancing Acts. *Cell* [online]. 2004, **117**(3), 285-297 [cit. 2023-01-05]. ISSN 00928674. doi:10.1016/S0092-8674(04)00343-5

[21] AROSIO, Paolo, Rosaria INGRASSIA a Patrizia CAVADINI. Ferritins: A family of molecules for iron storage, antioxidation and more. *Biochimica et Biophysica Acta (BBA) - General Subjects* [online]. 2009, **1790**(7), 589-599 [cit. 2023-01-05]. ISSN 03044165. doi:10.1016/j.bbagen.2008.09.004

[22] LAW, John H. Insects, Oxygen, and Iron. *Biochemical and Biophysical Research Communications* [online]. 2002, **292**(5), 1191-1195 [cit. 2023-01-05]. ISSN 0006291X. doi:10.1006/bbrc.2001.2015

[23] ANDREWS, Simon C. *Iron Storage in Bacteria* [online]. Elsevier, 1998, **40**, 281-351 [cit. 2023-01-19]. Advances in Microbial Physiology. ISBN 9780120277407. doi:10.1016/S0065-2911(08)60134-4

[24] ANDREWS, Simon, Andrea ROBINSON a Francisco RODRÍGUEZ-QUIñONES. Bacterial iron homeostasis. *FEMS Microbiology Reviews* [online]. 2003, **27**(2-3), 215-237 [cit. 2023-01-19]. ISSN 1574-6976. doi:10.1016/S0168-6445(03)00055-X

[25] ANDREWS, Simon C. The Ferritin-like superfamily: Evolution of the biological iron storeman from a rubrerythrin-like ancestor. *Biochimica et Biophysica Acta (BBA) - General Subjects* [online]. 2010, **1800**(8), 691-705 [cit. 2023-01-19]. ISSN 03044165. doi:10.1016/j.bbagen.2010.05.010

[26] ANDREWS, Simon, Nick BRUN, Vladimir BARYNIN, Andrew THOMSON, Geoffrey MOORE, John GUEST a Pauline HARRISON. Site-directed Replacement of the Coaxial Heme Ligands of Bacterioferritin Generates Heme-free Variants. *Journal of Biological Chemistry* [online]. 1995, **270**(40), 23268-23274 [cit. 2023-01-19]. ISSN 00219258. doi:10.1074/jbc.270.40.23268

[27] EBRAHIMI, Kourosh, Peter-Leon HAGEDOORN a Wilfred HAGEN. A Conserved Tyrosine in Ferritin Is a Molecular Capacitor. *ChemBioChem* [online]. 2013, **14**(9), 1123-1133 [cit. 2023-01-19]. ISSN 14394227. doi:10.1002/cbic.201300149

[28] CHIANCONE, Emilia, Andrea ILARI, Simonetta STEFANINI a Demetrius TSERNOGLOU. The dodecameric ferritin from Listeria innocua contains a novel intersubunit iron-binding site. *Nature Structural Biology* [online]. 2000, **7**(1), 38-43 [cit. 2023-02-10]. ISSN 10728368. doi:10.1038/71236

[29] HAIKARAINEN, Teemu a Anastassios PAPAGEORGIOU. Dps-like proteins: structural and functional insights into a versatile protein family. *Cellular and Molecular Life Sciences* [online]. 2010, **67**(3), 341-351 [cit. 2023-01-19]. ISSN 1420-682X. doi:10.1007/s00018-009-0168-2

[30] CARRONDO, M. A. NEW EMBO MEMBER'S REVIEW: Ferritins, iron uptake and storage from the bacterioferritin viewpoint. *The EMBO Journal* [online]. 2003, **22**(9), 1959-1968 [cit. 2023-01-19]. ISSN 14602075. doi:10.1093/emboj/cdg215

[31] CRICHTON, Robert. *Inorganic Biochemistry of Iron Metabolism: From Molecular Mechanisms to Clinical Consequences* [online]. Second Edition. American Chemical Society: John Wiley & Sons, 2001 [cit. 2023-01-27]. ISBN 9780470845790. 10.1002/0470845791

[32] LE BRUN, Nick, Allister CROW, Michael MURPHY, A. MAUK a Geoffrey MOORE. Iron core mineralisation in prokaryotic ferritins. *Biochimica et Biophysica Acta (BBA) - General Subjects* [online]. 2010, **1800**(8), 732-744 [cit. 2023-01-19]. ISSN 03044165. doi:10.1016/j.bbagen.2010.04.002

[33] LEVI, S, A LUZZAGO, F FRANCESCHINELLI, P SANTAMBROGIO, G CESARENI a P AROSIO. Mutational analysis of the channel and loop sequences of human ferritin H-chain. *Biochemical Journal* [online]. 1989, **264**(2), 381-388 [cit. 2023-01-19]. ISSN 0264-6021. doi:10.1042/bj2640381

[34] WALDEN, William, Anna SELEZNEVA, Jérôme DUPUY, Anne VOLBEDA, Juan FONTECILLA-CAMPS, Elizabeth THEIL a Karl VOLZ. Structure of Dual Function Iron Regulatory Protein 1 Complexed with Ferritin IRE-RNA. *Science* [online]. 2006, **314**(5807), 1903-1908 [cit. 2023-01-06]. ISSN 0036-8075. doi:10.1126/science.1133116

[35] HARRISON, Pauline M. a Paolo AROSIO. The ferritins: molecular properties, iron storage function and cellular regulation. *Biochimica et Biophysica Acta (BBA) - Bioenergetics* [online]. 1996, **1275**(3), 161-203 [cit. 2023-02-12]. ISSN 00052728. doi:10.1016/0005-2728(96)00022-9

[36] TOUSSAINT, Louise, Luc BERTRAND, Louis HUE, Robert R. CRICHTON a Jean-Paul DECLERCQ. High-resolution X-ray Structures of Human Apoferritin H-chain Mutants Correlated with Their Activity and Metal-binding Sites. *Journal of Molecular*

Biology [online]. 2007, **365**(2), 440-452 [cit. 2023-01-19]. ISSN 00222836. doi:10.1016/j.jmb.2006.10.010

[37] GRANIER, T., B. GALLOIS, A. DAUTANT, B. LANGLOIS D'ESTAINTOT a G. PRÉCIGOUX. Comparison of the Structures of the Cubic and Tetragonal Forms of Horse-Spleen Apoferritin. *Acta Crystallographica Section D Biological Crystallography* [online]. 1997, **53**(5), 580-587 [cit. 2023-01-19]. ISSN 0907-4449. doi:10.1107/S0907444997003314

[38] HA, Y., Dashuang SHI, George W. SMALL, Elizabeth C. THEIL a N. M. ALLEWELL. Crystal structure of bullfrog M ferritin at 2.8 Å resolution: analysis of subunit interactions and the binuclear metal center. *JBIC Journal of Biological Inorganic Chemistry* [online]. 1999, **4**(3), 243-256 [cit. 2023-01-19]. ISSN 0949-8257. doi:10.1007/s007750050310

[39] HAMBURGER, Agnes E., Anthony P. WEST, Zsuzsa A. HAMBURGER, Peter HAMBURGER a Pamela J. BJORKMAN. Crystal Structure of a Secreted Insect Ferritin Reveals a Symmetrical Arrangement of Heavy and Light Chains. *Journal of Molecular Biology* [online]. 2005, **349**(3), 558-569 [cit. 2023-01-19]. ISSN 00222836. doi:10.1016/j.jmb.2005.03.074

[40] MASUDA, Taro, Fumiyuki GOTO, Toshihiro YOSHIHARA a Bunzo MIKAMI. Crystal Structure of Plant Ferritin Reveals a Novel Metal Binding Site That Functions as a Transit Site for Metal Transfer in Ferritin. *Journal of Biological Chemistry* [online]. 2010, **285**(6), 4049-4059 [cit. 2023-01-19]. ISSN 00219258. doi:10.1074/jbc.M109.059790

[41] STILLMAN, T.J, P.D HEMPSTEAD, P.J ARTYMIUK, S.C ANDREWS, A.J HUDSON, A TREFFRY, J.R GUEST a P.M HARRISON. The high-resolution X-ray crystallographic structure of the ferritin (EcFtnA) of Escherichia coli; comparison with human H ferritin (HuHF) and the structures of the Fe3 and Zn2 derivatives11Edited by R. Huber. *Journal of Molecular Biology* [online]. 2001, **307**(2), 587-603 [cit. 2023-01-19]. ISSN 00222836. doi:10.1006/jmbi.2001.4475

[42] CRICHTON, Robert R. a Jean-Paul DECLERCQ. X-ray structures of ferritins and related proteins. *Biochimica et Biophysica Acta (BBA) - General Subjects* [online]. 2010, **1800**(8), 706-718 [cit. 2023-01-25]. ISSN 03044165. doi:10.1016/j.bbagen.2010.03.019

[43] BERTINI, Ivano, Daniela LALLI, Stefano MANGANI, Cecilia POZZI, Camilla ROSA, Elizabeth C. THEIL a Paola TURANO. Structural Insights into the Ferroxidase Site of Ferritins from Higher Eukaryotes. *Journal of the American Chemical Society* [online]. 2012, **134**(14), 6169-6176 [cit. 2023-01-27]. ISSN 0002-7863. doi:10.1021/ja210084n

[44] FUNK, Felix, Jean-Pierre LENDERS, Robert R. CRICHTON a Walter SCHNEIDER. Reductive mobilisation of ferritin iron. *European Journal of Biochemistry* [online]. 1985, **152**(1), 167-172 [cit. 2023-01-27]. ISSN 0014-2956. doi:10.1111/j.1432-1033.1985.tb09177.x

[45] SIRIVECH, Somjai, Earl FRIEDEN a Shigemasa OSAKI. The release of iron from horse spleen ferritin by reduced flavins. *Biochemical Journal* [online]. 1974, **143**(2), 311-315 [cit. 2023-01-27]. ISSN 0264-6021. doi:10.1042/bj1430311

[46] WATT, G D, D JACOBS a R B FRANKEL. Redox reactivity of bacterial and mammalian ferritin: is reductant entry into the ferritin interior a necessary step for iron release?. *Proceedings of the National Academy of Sciences* [online]. 1988, **85**(20), 7457-7461 [cit. 2023-01-27]. ISSN 0027-8424. doi:10.1073/pnas.85.20.7457

[47] HAJDUSEK, Ondrej, Daniel SOJKA, Petr KOPACEK, Veronika BURESOVA, Zdenek FRANTA, Ivo SAUMAN, Joy WINZERLING a Libor GRUBHOFFER. Knockdown of proteins involved in iron metabolism limits tick reproduction and development. *Proceedings of the National Academy of Sciences* [online]. 2009, **106**(4), 1033-1038 [cit. 2022-05-25]. ISSN 0027-8424. doi:10.1073/pnas.0807961106

[48] KOPÁČEK, Petr, Jana ŽDYCHOVÁ, Toyoshi YOSHIGA, Christoph WEISE, Natasha RUDENKO a John LAW. Molecular cloning, expression and isolation of ferritins from two tick species—Ornithodoros moubata and Ixodes ricinus. *Insect*

Biochemistry and Molecular Biology [online]. 2003, **33**(1), 103-113 [cit. 2022-05-25]. ISSN 0965-1748. doi:https://doi.org/10.1016/S0965-1748(02)00181-9

[49] LARA, Flavio, Ulysses LINS, Gabriela PAIVA-SILVA, Igor ALMEIDA, Cláudia BRAGA, Flávio MIGUENS, Pedro OLIVEIRA a Marílvia DANSA-PETRETSKI. A new intracellular pathway of haem detoxification in the midgut of the cattle tick Boophilus microplus: aggregation inside a specialized organelle, the hemosome. *J Exp Biol* [online]. 2003, **206**(10), 1707-1715 [cit. 2023-01-05]. https://doi.org/10.1242/jeb.00334

[50] HAJDUSEK, Ondrej, Consuelo ALMAZÁN, Gabriela LOOSOVA, Margarita VILLAR, Mario CANALES, Libor GRUBHOFFER, Petr KOPACEK a José DE LA FUENTE. Characterization of ferritin 2 for the control of tick infestations. *Vaccine* [online]. 2010, **28**(17), 2993-2998 [cit. 2023-01-06]. ISSN 0264410X. doi:10.1016/j.vaccine.2010.02.008

[51] DE MEULENAERE, Evelien, Jake Brian BAILEY, Faik Akif TEZCAN a Dimitri Dominique DEHEYN. First biochemical and crystallographic characterization of a fast-performing ferritin from a marine invertebrate. *Biochemical Journal* [online]. 2017, **474**(24), 4193-4206 [cit. 2023-03-27]. ISSN 0264-6021. doi:10.1042/BCJ20170681

[52] ZHAO, Yu, Lei LIU, Jin-Bao LIU, Cong-Ying WU, De-Yong DUAN a Tian-Yin CHENG. Cloning, expression, and function of ferritins in the tick Haemaphysalis flava. *Ticks and Tick-borne Diseases* [online]. 2022, **13**(2) [cit. 2023-03-27]. ISSN 1877959X. doi:10.1016/j.ttbdis.2021.101892

[53] MASUDA, Taro, Jiachen ZANG, Guanghua ZHAO a Bunzo MIKAMI. The first crystal structure of crustacean ferritin that is a hybrid type of H and L ferritin. *Protein Science* [online]. 2018, **27**(11), 1955-1960 [cit. 2023-03-27]. ISSN 09618368. doi:10.1002/pro.3495

[54] LI, Kunpeng, Thomas KLOSE, Chen SUN, Yue LIU a Wen JIANG. 2.5 Å Resolution Cryo-EM Structure of Human Apo-ferritin Using an Optimized Workflow for Volta

Phase Plate. *Microscopy and Microanalysis* [online]. 2018, **24**(1), 900-901 [cit. 2023-03-30]. ISSN 1431-9276. doi:10.1017/S1431927618004993

[55] LUNDIN, Daniel, Anthony M. POOLE, Britt-Marie SJÖBERG a Martin HÖGBOM. Use of Structural Phylogenetic Networks for Classification of the Ferritin-like Superfamily. *Journal of Biological Chemistry* [online]. 2012, **287**(24), 20565-20575 [cit. 2023-01-19]. ISSN 00219258. doi:10.1074/jbc.M112.367458

[56] GRANIER, Thierry, Béatrice LANGLOIS D'ESTAINTOT, Bernard GALLOIS, Jean-Marc CHEVALIER, Gilles PRÉCIGOUX, Paolo SANTAMBROGIO a Paolo AROSIO. Structural description of the active sites of mouse L-chain ferritin at 1.2 Å resolution. *JBIC Journal of Biological Inorganic Chemistry* [online]. 2003, **8**(1), 105-111 [cit. 2023-01-25]. ISSN 0949-8257. doi:10.1007/s00775-002-0389-4

[57] JIANG, Bing, Long FANG, Kongming WU, Xiyun YAN a Kelong FAN. Ferritins as natural and artificial nanozymes for theranostics. *Theranostics* [online]. 2020, **10**(2), 687-706 [cit. 2023-02-12]. ISSN 1838-7640. doi:10.7150/thno.39827

[58] YÉVENES, Alejandro. The Ferritin Superfamily. *Macromolecular Protein Complexes* [online]. Cham: Springer International Publishing, 2017, **83**, 75-102 [cit. 2023-02-14]. Subcellular Biochemistry. ISBN 978-3-319-46501-2. doi:10.1007/978-3-319-46503-6_3

[59] ELAD, Nadav, Giuliano BELLAPADRONA, Lothar HOUBEN, Irit SAGI a Michael ELBAUM. Detection of isolated protein-bound metal ions by single-particle cryo-STEM. *Proceedings of the National Academy of Sciences* [online]. 2017, **114**(42), 11139-11144 [cit. 2023-03-30]. ISSN 0027-8424. doi:10.1073/pnas.1708609114

[60] IRIMIA-DOMINGUEZ, Jose, Chen SUN, Kunpeng LI et al. Cryo-EM structures and functional characterization of homo- and heteropolymers of human ferritin variants. *Scientific Reports* [online]. 2020, **10**(1) [cit. 2023-03-30]. ISSN 2045-2322. doi:10.1038/s41598-020-77717-4

[61] NAYDENOVA, Katerina, Mathew J. PEET a Christopher J. RUSSO. Multifunctional graphene supports for electron cryomicroscopy. *Proceedings of the National Academy of Sciences* [online]. 2019, **116**(24), 11718-11724 [cit. 2023-04-03]. ISSN 0027-8424. doi:10.1073/pnas.1904766116

7 List of figures

8 List of tables

9 Supplements

9.1 Cleavage reporter sequences of ferritin II

DNA sequence:

ATTTTTCAGACGCACGAAAGACAGATCAGCACCCGCTCGATCCACATCCATCA
TGAAGCAATTTGTGGTCATCCTTGCGCTCATCGGCGCAGCGACGTCAGGGAAC
AATTTGTTCGAAAACCTGGACAAGTACCCGCTTCAAGATGAATGTCAAGCAGC
GCTGCAGGAACACATCAATGTCGAAATGCACGCAAGCCTCGTATATATGCAGA
TGGCGGCACACTTCGACAACAACAAAGTGGCTCGGAAGGGTTTCAGTACTTTC
TTTGCCGAGAACTCCAAAGAGGAACGTGAGCACGCCCAAAAGATCATCGACTA
CATCAACAAGAGGGGCAGCACCGTCTCGCTCGTCAATATCGACATGCCCCTGA
TCACCACTTGGAAATCCGTTTTGCAAGCGCTGCGAGATGCCATCAGCTTGGAG
AACAAAGTGACCAACAAGCTCCACGCCGTGCACAAGATTGCCGATGAGGAGT
GCAAAGACCCTCAGCTCATGGACTTCATCGAGAGCGAGTTCTTGGAGGAGCAA
GTGAATTCCATTGACAAGCTGCAGCGAATGATTACAGTACTCAGTAACATGGA
CTCCGGCACGGGGGAGTACCTGTTGGACAGAGAGCTGCTCGGAGACAAGAAG
GAATTTTAAGCACTTGCTTTTCAGTAGAATCCCAATTCCCAAGGCGTGTCGCTG
GGTCGGCGACAAATCAAGGTGTATTGAAGGACTCAAACTGCAAGAAACACTTT
CTGGTTGCCTAGAAAACATTCATATGTATTGGTTAAACGCTTCAAAACTTTCCC
TATCCCAACTATCCTATTTGTTTTCAAAACTTCCCACTGATTTTAGTTTTGACGA
ATTCTGGGGAGCAGGGGCATCTGTTGCAATAAAAGGTCAAACGACAGCAAAA
AAAAAAAAAAAAAAAAAAAAAAAAA

Protein sequence:

MKQFVVILALIGAATSGNNLFENLDKYPLQDECQAALQEHINVEMHASLVYMQM
AAHFDNNKVARKGFSTFFAENSKEEREHAQKIIDYINKRGSTVSLVNIDMPLITTW
KSVLQALRDAISLENKVTNKLHAVHKIADEECKDPQLMDFIESEFLEEQVNSIDKL
QRMITVLSNMDSGTGEYLLDRELLGDKKEF

Theoretical molecular weight: 24,833 kDa

Theoretical pI: 5,35

Molar extinction coefficient: 11 585

9.2 Used solutions

Table 15: List of all used solutions with their composition

Solution	Composition
50x TAE (diluted in H_2O for 1x TAE)	246 g Tris, 57.1 ml acetic acid, 100 ml 0,5M EDTA in 1 l dH_2O
Lysis buffer	50 mM potassium phosphate, 400 mM NaCl, 100 mM KCl, 10% glycerol, 0,5% TritonX-100, pH 7.8
4x Laemmli buffer	20 ml of 0.5 M Tris, 4 g SDS, 20 ml of glycerol, 0.1 of bromphenol blue, dH_2O up to 45 ml, pH 6.8
4x SDS-PAGE sample buffer	900 µl of 4x Laemmli buffer and 100 µl of β-mercaptoethanol
1x SDS-PAGE sample buffer	Dilution of 4x SDS-pAFE sample buffer in 1x PBS
10x SDS-PAGE running buffer (diluted in H_2O for 1x SDS-PAGE running buffer)	250 mM Tris, 1.92 M glycine, 1% SDS
Fixing solution	50% ethanol, 2% phosphoric acid
Staining solution	1,2g Coomassie Blue G-250, 23.4 ml phosphoric acid, 100g ammonium sulfate in 800 ml of dH_2O, 200 ml 100% methanol
10x transfer buffer (diluted in H_2O for 1x transfer buffer)	58.15g Tris, 29.3g glycine, 3.75g SDS in 1l dH_2O
10x TBS buffer	60.5g Tris, 87.66g NaCl in 1l dH_2O, pH=7.6
1x TBS-T	100 ml of 10x TBS buffer in 1l dH_2O, 1 ml Tween20

9.3 pET100 vector – primers

Table 16: Designed primers for pET100 vector from the Laboratory of Molecular Biology of Ticks, IOP

Vector	Primer	Sequence (5'-3')	Length [bp]
pET100	Fer2-Exp-F	CACCGGGAACAATTTGTTCGAAAAC	25
	Fer2-Exp-R	GCAAGTGCTTAAAACTCCTTCTTG	24

9.4 Results

9.4.1 Colony PCR

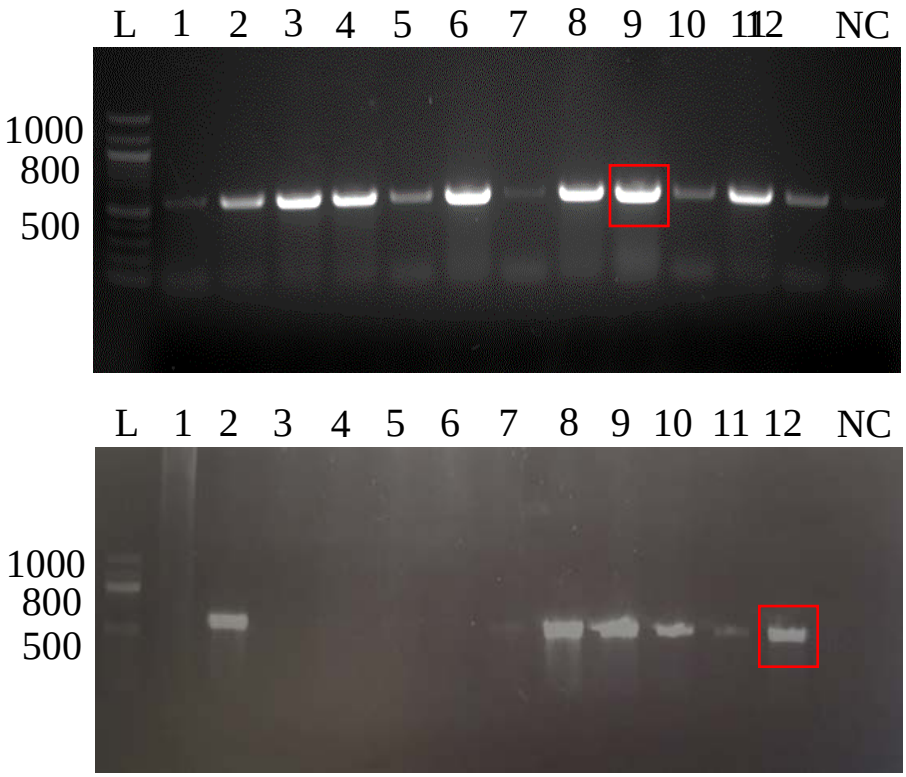

Figure 27: **Colony PCR of pET21d (upper part) and pASK-IBA33+ (bottom part):** For pET21d vector, colony 11 was used for further studies. Colony 12 was chosen for pASK3IBA33+. L – 100 bp DNA ladder, 1-12 – selective colonies, NC – negative control with no DNA template, red box – picked colonies

9.4.2 Pilot expression

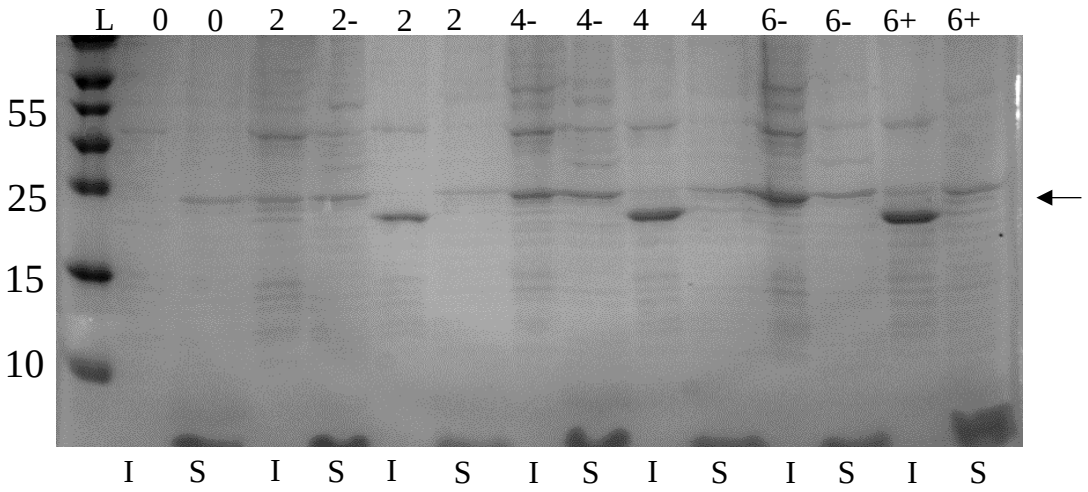

Figure 28: **Pilot expression of ferritin II in pASK-IBA37+** in BL21-CodonPlus cells at 37 °C induced by ATC. L - PageRulerTM Protein Prestained Ladder, number – an hour of harvesting, - uninduced culture, + induced culture, I – insoluble fraction, S – soluble fraction

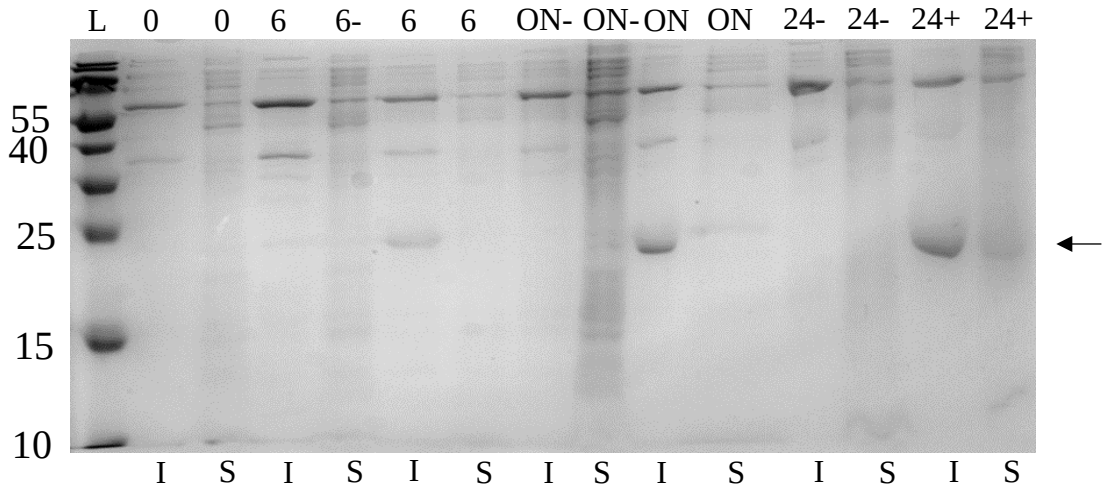

Figure 29: **Pilot expression of ferritin II in pASK-IBA37+** in ArticExpress(DE3) cells at 13 °C induced by ATC. L - PageRulerTM Protein Prestained Ladder, number – an hour of harvesting, ON – overnight, -uninduced culture, + induced culture, I – insoluble fraction, S – soluble fraction

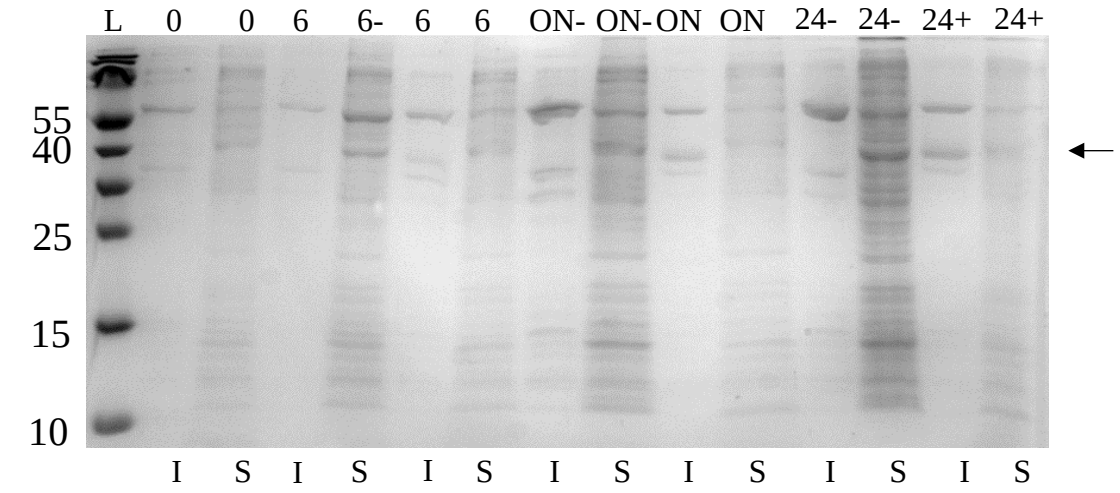

Figure 30: **Pilot expression of ferritin II in pETSUMO** in ArticExpress(DE3) cells at 13 °C induced by 1 mM IPTG. L - PageRulerTM Protein Prestained Ladder, number – an hour of harvesting, ON – overnight, - uninduced culture, + induced culture, I – insoluble fraction, S – soluble fraction

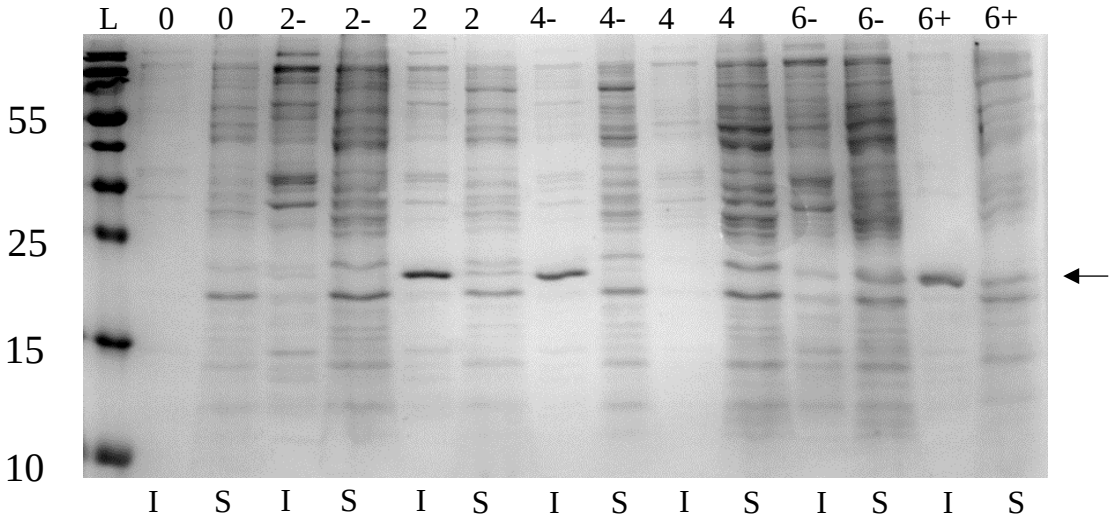

Figure 31: **Pilot expression of ferritin II in pASK-IBA37+** in Rosetta^{TM}(DE3) cells at 37 °C induced by ATC. L - PageRulerTM Protein Prestained Ladder, number – an hour of harvesting, -uninduced culture, + induced culture, I – insoluble fraction, S – soluble fraction

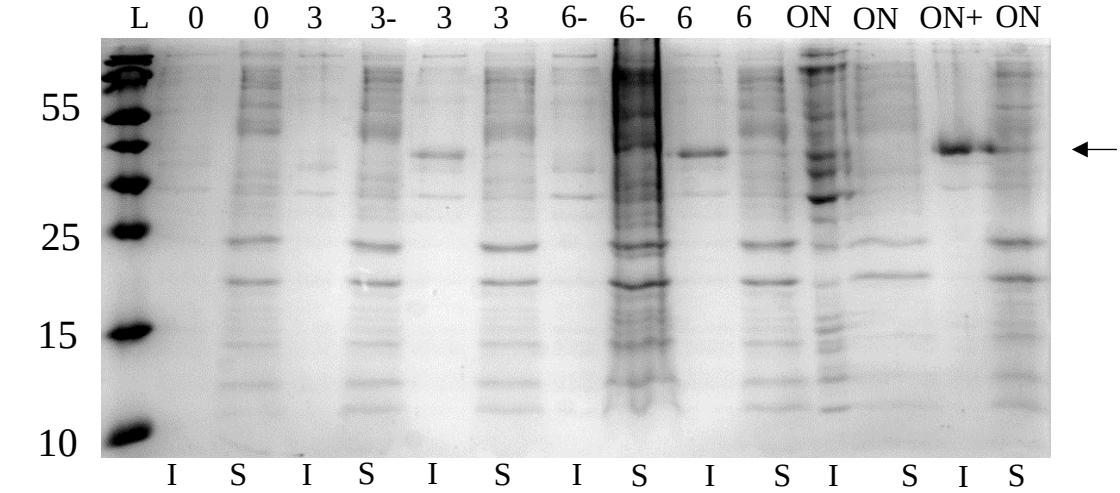

Figure 32: **Pilot expression of ferritin II in pETSUMO** in Rosetta^{TM}(DE3) cells at 18 °C induced by 1 mM IPTG. L - PageRulerTM Protein Prestained Ladder, number – an hour of harvesting, ON – overnight, -uninduced culture, + induced culture, I – insoluble fraction, S – soluble fraction

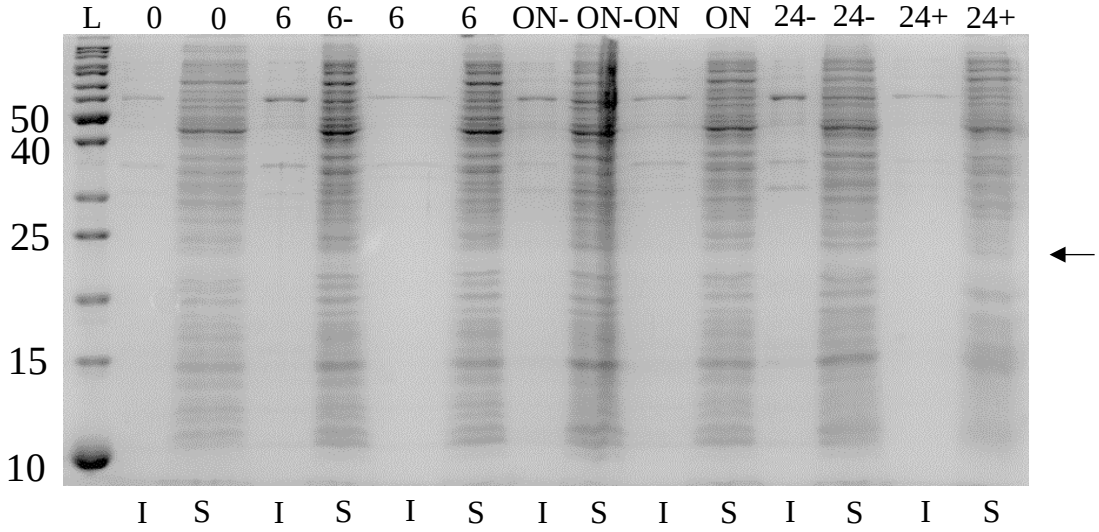

Figure 33: **Pilot expression of ferritin II in pET21d** in ArticExpress(DE3) cells at 13 °C induced by 1 mM IPTG. L - PageRulerTM Protein Prestained Ladder, number – an hour of harvesting, ON – overnight, - uninduced culture, + induced culture, I – insoluble fraction, S – soluble fraction

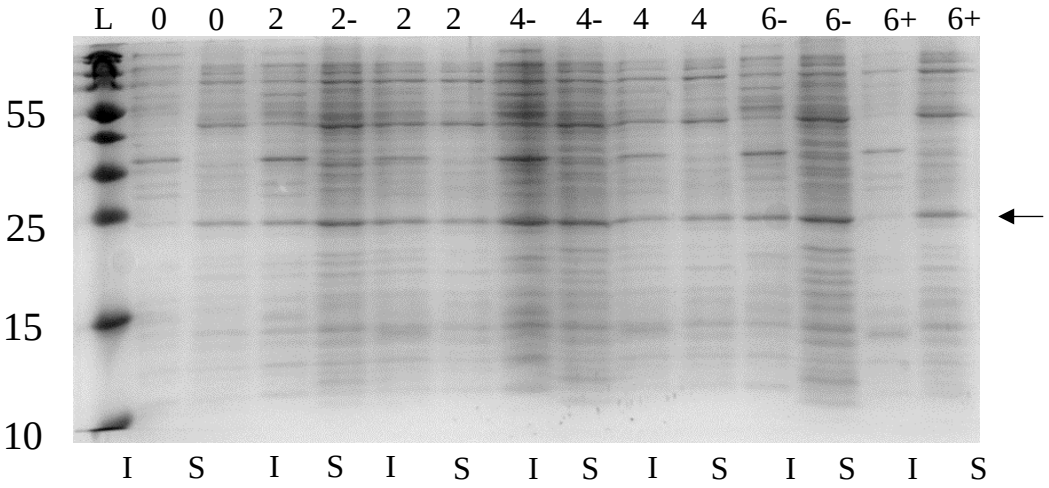

Figure 34: **Pilot expression of ferritin II in pET21d** in BL21-CodonPlus cells at 37 °C induced by 0,5 mM IPTG. L - PageRulerTM Protein Prestained Ladder, number – an hour of harvesting, - uninduced culture, + induced culture, I – insoluble fraction, S – soluble fraction

9.4.3 Results from size-exclusion chromatography

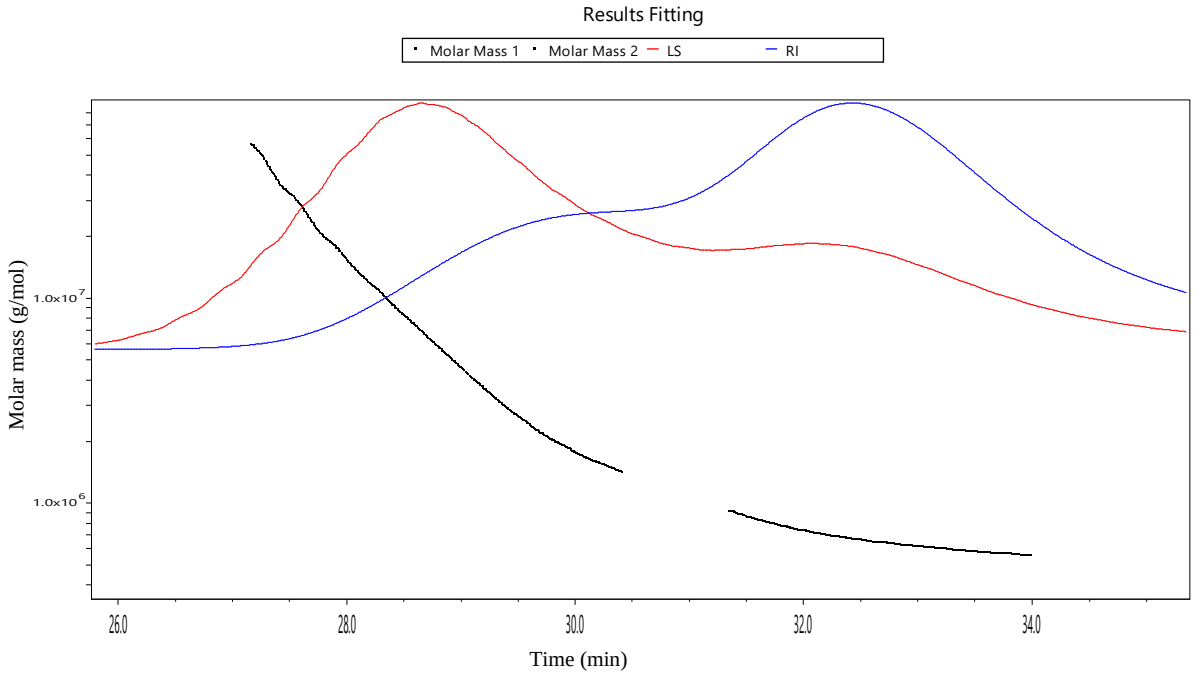

Figure 35: **Results fitting of homogeneity from size-exclusion chromatography** with SEC200 10/300 GL column